Proposal to participate in the first measurement of θ_{13}: The Double Chooz Experiment

October 25, 2006

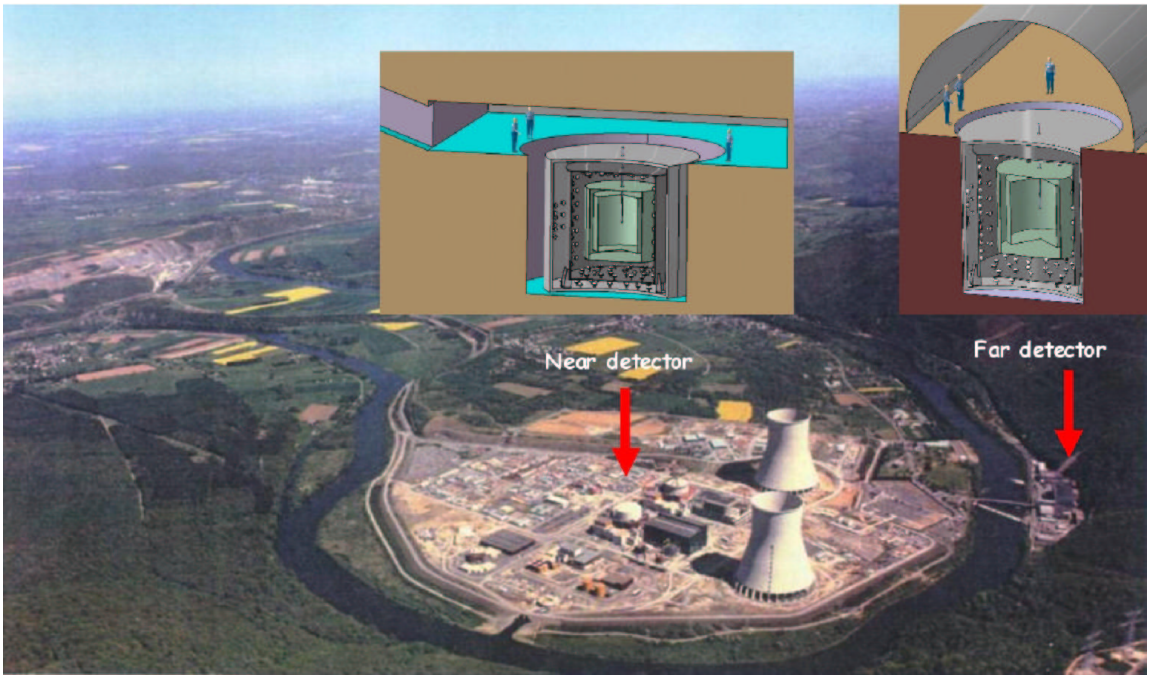

S.Berridge[1], A.Bernstein[2], T.Bolton[3], N.S.Bowden[4], B.Bugg[1], J.Busenitz[5], H.Cohn[1], J.Coleman[6], S.Dazeley[2,11], Y.Efremenko[1], T.Gabriel[1], M.Goodman[7], T.Handler[1], G.Horton-Smith[3], Y.Kamyshkov[1], D.M.Kaplan[8], C.Lane[9], Y.Liu[5], J.LoSecco[10], J.Maricic[9], D.McKee[5], W.Metcalf[6], J.Reichenbacher[7], D.Reyna[7], H.Rubin[8], I.Stancu[5], N.Stanton[3], R.Svoboda[2,11], A.Tang[3]

1. The University of Tennessee
2. Lawrence Livermore National Laboratory
3. Kansas State University
4. Sandia National Laboratory
5. The University of Alabama
6. Louisiana State University
7. Argonne National Laboratory
8. Illinois Institute of Technology
9. Drexel University
10. The University of Notre Dame
11. The University of California, Davis

Contents

1 The Double Chooz Experiment **7**
1.1 Overview . . . 7
1.2 Experimental site: the Chooz nuclear reactors . . . 9
1.3 Time scale . . . 11
1.4 The Collaboration . . . 11
1.5 The Double Chooz Detector Concept . . . 13
1.6 Physics Reach . . . 14
1.6.1 Signal . . . 14
1.6.2 Experimental errors . . . 16
1.6.3 Backgrounds . . . 17
1.6.4 Sensitivity . . . 24
1.7 Detector Structures and Materials . . . 25
1.7.1 Detector dimensions . . . 25
1.7.2 PMT support structure . . . 26
1.7.3 Scintillator and Buffer Liquid . . . 27
1.8 Phototubes . . . 30
1.8.1 PMT Performance . . . 31
1.8.2 Sensitivity to Magnetic Field . . . 31

2 Budget **34**
2.1 Overview of Costs . . . 34
2.2 Work Breakdown Structure (WBS) . . . 34
2.3 Cost & Schedule Details . . . 36
2.4 Project Management . . . 37

3 Calibration **40**
3.1 Calibration Goals . . . 40
3.2 Radioactive Sources . . . 41
3.2.1 Gamma Sources . . . 41
3.2.2 Neutron Sources . . . 42
3.2.3 Fabrication of Radioactive Sources . . . 45
3.3 Laser Flashers . . . 46
3.3.1 General Description . . . 46
3.3.2 System Description . . . 47
3.4 Calibration Deployment . . . 48
3.4.1 Deployment Methods Overview . . . 49
3.4.2 z-Axis System . . . 49
3.4.3 Articulated Arm . . . 49
3.4.4 Laser Fiber Windlass . . . 50
3.4.5 Source Tube and Wire Drivers . . . 50
3.5 Detector Interface . . . 51
3.5.1 Glovebox fabrication . . . 52
3.5.2 Clean rooms . . . 52

3.6 Calibration and Monitoring Plan 52

4 Electronics **54**
4.1 High Voltage System 54
4.2 HV splitter 56
4.3 Front-End Electronics 59
4.4 Slow Monitoring 68
4.5 PMT Rate Monitor 72

5 Radiopurity Assessment **74**
5.1 Comparison with Chooz 74
5.2 Activity of Materials 74
5.3 Check with a Detailed MC 77
5.4 Radiopurity Monitoring 78

Contact Information

Contact Person/PI:	Prof. Robert Svoboda Department of Physics University of California, Davis 1 Shields Ave Davis, CA 95616 *rsvoboda@physics.ucdavis.edu*
Dept of Energy Contact:	P.K.Williams Research and Technology Division, SC-25.1

Executive Summary

It is widely recognized that the potential of reactor anti-neutrino experiments has not been fully exploited. High precision neutrino oscillation measurements can be made by a multi-detector experiment where many uncertainties associated with reactor power, neutrino yield, and interaction cross-sections can in principle be made negligibly small. This strategy has been adopted by the Double Chooz collaboration in order to search for a non-vanishing value of θ_{13}. This is a crucial parameter in determining the feasibility of the next generation of experiments to determine the neutrino mass hierarchy and search for CP violation in the lepton sector. A question of paramount importance to the High Energy Physics community is how many resources to devote to new generation of neutrino experiments in context of a need to support ILC development. Double Chooz will provide the information necessary to make an informed priority decision on a time scale significantly faster than any other experiment.

The current best direct limit on θ_{13} comes from the Chooz reactor experiment which ran in 1997-98. This experiment was not designed to measure θ_{13} but rather to look for $\nu_e \rightarrow \nu_x$ oscillations that could explain the atmospheric neutrino anomaly. The Double Chooz initiative started in the summer of 2003 with the realization that the original Chooz experiment could be significantly improved on a rapid time scale and at low cost by adding a second detector close in, improving the detector design, and simply running longer. The existing neutrino far lab located 300 m.w.e. underground 1.05 km from two N4-class reactors is immediately available with almost no refurbishment required. There is enthusiastic support from Electricité de France, which has provided a site and engineering design support for an 80 m.w.e. deep near lab on the reactor site.

Internationally, there are two other reactor neutrino projects under review: (1) The Daya Bay project in China, and (2) the RENO project in Korea. We believe that the advanced stage of Double Chooz planning and development and the use of existing facilities makes Double Chooz almost certain to be the first experiment to have a chance to measure a non-zero θ_{13}. Double Chooz will limit $\sin^2 2\theta_{13}$ to 0.022-0.030 (for $\Delta m^2 = 3.5 - 2.5 \times 10^{-3} eV^2$). If θ_{13} is below this range, first generation long-baseline accelerator experiments will have almost no capability to address the mass hierarchy or CP violation questions. The Double Chooz far detector will begin operation in early 2008 followed by the near detector in mid-2009.

Double Chooz will also lay the foundation for future experiments requiring high precision through the development of innovative technologies (scintillator, identical detectors, detector inter-calibration, etc.). There is considerable interest both in the U.S. (NNSA) and in France (Saclay) in developing these technologies for use in voluntary monitoring of plutonium production in civilian nuclear power plants. In the U.S. we currently tap into this parallel development stream via our collaborators at LLNL and SNL, who operate an existing NNSA-sponsored anti-neutrino detector at the San Onofre Nuclear Generating Station. This type of technological co-investment is unique to Double Chooz and is a result of the historically close cooperation between France and the U.S. in this area.

The Double Chooz experiment was approved by the French scientific councils of CEA-DSM-DAPNIA and CNRS-IN2P3 in 2004. Funding has now started and work has begun in the far lab site to prepare it for shield installation later this year. In addition, the Max Planck Society has approved funding for the scintillator and related handling systems starting this year and purchasing for these items has started. A group of German universities is awaiting final approval from the Deutsche Forschungsgemeinschaft (DFG) to build the inner veto. Funding for the groups in Spain and Russia has been approved. Thus the funding situation in Europe is essentially in place. Construction was started at the far site in June, 2006.

In addition to strong European support, there is now also a request from the former KASKA group in Japan to join Double Chooz. A proposal for their participation has been submitted to the Japanese funding agencies. The prospects for approval are very good.

In the U.S. there are both NSF and DOE supported groups working on Double Chooz. The NSF supported groups (Chicago and Columbia) have been awarded R&D funding to design a muon tracking system. They will submit a full construction request to the NSF his Fall. The DOE-supported groups have designed the analog electronics, calibration, and monitoring systems for the experiment. This proposal is a request for the funding to construct those systems.

Since Double Chooz is a precision experiment limited by systematics, these systems are central to the final result of the experiment, but are relatively low cost components. Thus for a small amount of money we could have a major impact on the final results, capitalizing on the almost three years of planning and effort that have already gone into designing these systems since we helped to write the original 2003 European LOI.

Given the high level of interest in Double Chooz and the willingness of many countries to increase their participation, it is necessary for this proposal to be acted on as soon as possible if there is to be a significant role for U.S. DOE groups to work with their NSF-supported colleagues in making the first measurement of θ_{13}.

1 The Double Chooz Experiment

1.1 Overview

This is a proposal by an experienced collaboration of neutrino physicists to join an international effort to modify the existing neutrino physics facility at the Chooz-B nuclear power station in France[1, 2, 3]. The experiment, known as Double Chooz, is planned to reach a sensitivity to $\sin^2 2\theta_{13}$ down to 0.03 over a three year run during 2008–2011. This will cover roughly 85% of the currently allowed region. The costs and time to first results for this critical parameter can be minimized since our project takes advantage of an existing laboratory. This proposal describes the plan for U.S. participation in Double Chooz, and should be reviewed together with the 156 page full collaboration proposal [1] which can be can be obtained from http://www.arxiv.org/ as hep-ex/0606025.

The Double Chooz reactor neutrino experiment [1] offers the world particle physics community a relatively quick and inexpensive opportunity to measure the mixing angle θ_{13} if it is not too small: $\sin^2 2\theta_{13} > 0.03$. For $\Delta m^2 \approx 2.5 \times 10^{-3}\mathrm{eV}^2$, Double Chooz will be sensitive to 0.05 after 1 year of data taking and 0.03 or better after 3 years of operation with two detectors. If θ_{13} is in this range, long-baseline off-axis neutrino experiments may be able to measure matter effects and search for CP violation [4, 5, 6]. *On the other hand, if it is less than 0.03, then there is essentially no chance to resolve the mass hierarchy or CP questions without significant upgrades.* This is shown in Figures 1 and 2 which are from a recent Fermilab PAC presentation[7]. Figure 1 shows the percentage of possible δ_{CP} values for which the neutrino mass hierarchy can be resolved at the 95% CL as a function of $sin^2 2\theta_{13}$, assuming six years of running. The dashed red line is the current CHOOZ limit. If the value is less than 0.04, at least beam upgrades, and perhaps even megaton scale detectors will be required. Figure 2 shows a similar format for a 3σ resolution of δ_{CP}, except in this case a Proton Driver for FNAL and 4MW beam upgrade for T2K are assumed. It is clear that a value of $sin^2 2\theta_{13} < 0.04$ means that significantly more resources will have to be committed to solve this problem. On the other hand, a large value > 0.07 or so means a rich program with existing facilities. *Double Chooz is an experiment designed to provide an answer to this all-important question on the fastest possible time scale.*

This proposal is organized in three main sections. The first section is a brief description of the experiment - essentially a condensation of the Full Collaboration Proposal [1]. This includes a description of the site and detectors and a summary of the sensitivity and backgrounds. The second section presents the budget for the items requested in this proposal. These center around those systems that are most closely related to maintaining detector stability and controlling systematic uncertainties. These are:

- Calibrations (section 3)
- Analog Electronics (section 4.2 and section 4.3)

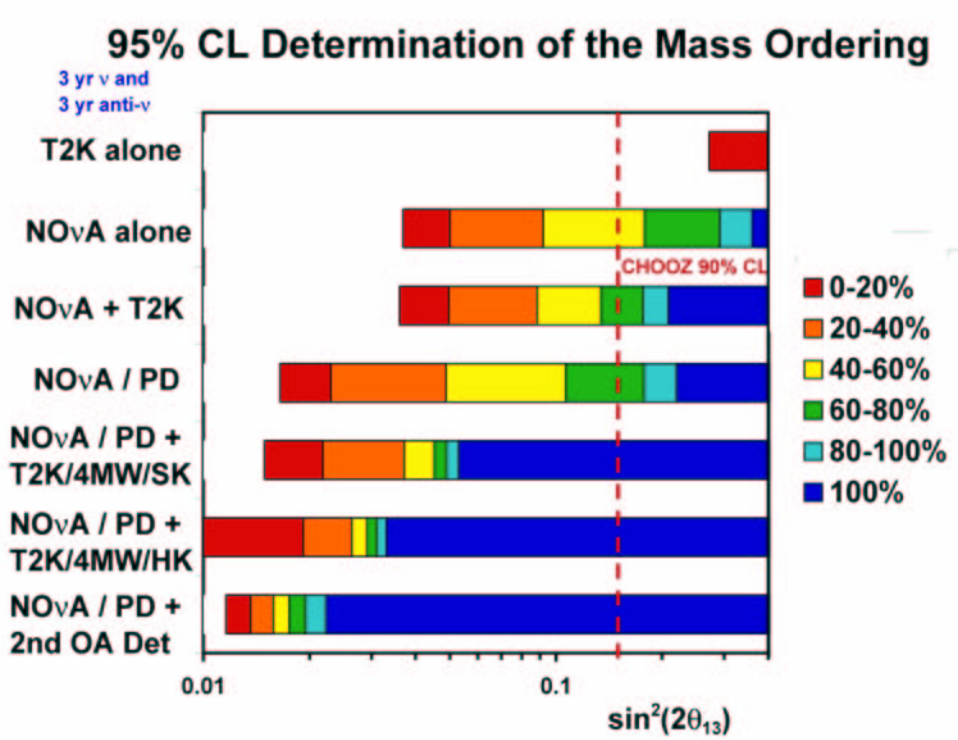

Figure 1: Fraction of δ_{CP} for which the neutrino mass hierarchy problem can be resolved at the 95% c.l. as a function of $sin^2 2\theta_{13}$. [7] Assumes six years of running by NOvA.

- Environmental Monitoring (section 4.4)
- Detector Monitoring (section 4.5)
- Radiopurity (section 5)

These items of scope are not costly, but represent some of the most crucial components of the experiment if Double Chooz is to reach its sensitivity goals. Total requested funds are $1.3M over four years.

The final three sections describe these systems in detail. As can be seen, significant progress has been made in the design and planning of the work we propose to accomplish with this proposal. Indeed, the U.S. DOE groups have been an integral part of the Double Chooz experiment since its inception in 2003 and have contributed greatly to its intellectual evolution and design maturity. We have played a major role in all areas of the experiment, including detector simulations, analysis of backgrounds, and studies of the reactor source and site. This proposal represents our desire to capitalize on these years of work and to participate in this important experiment, which will have such far-reaching consequences for the future of particle physics.

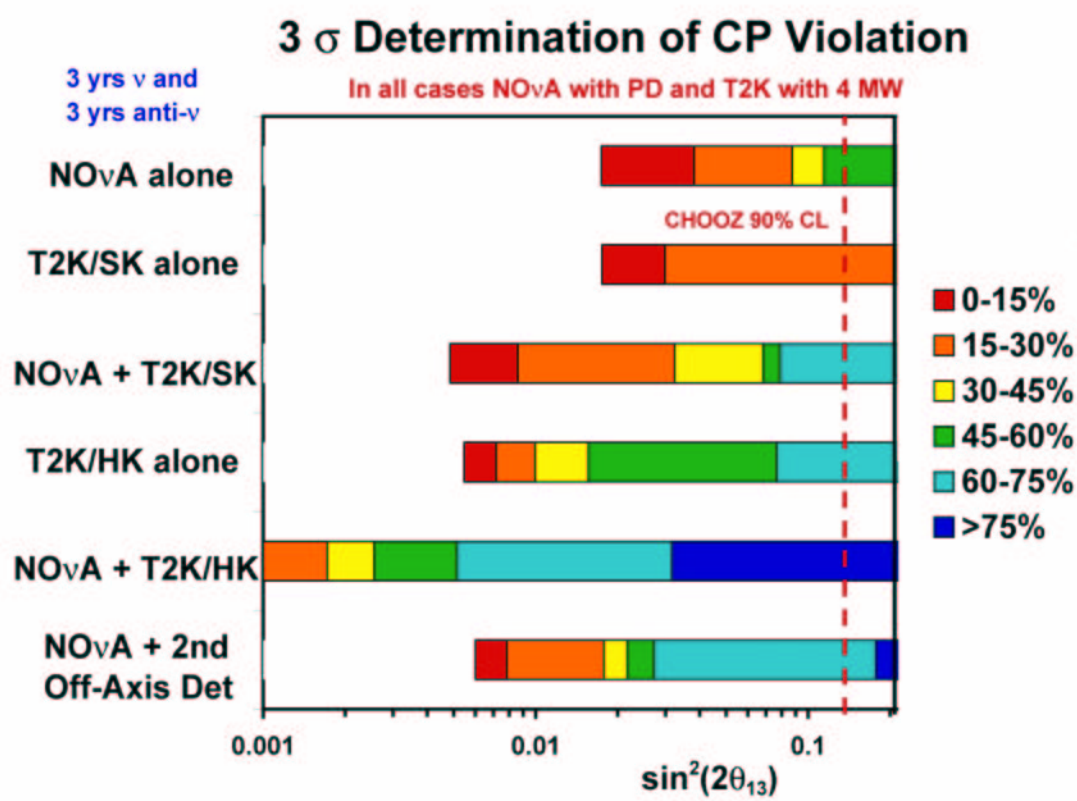

Figure 2: Fraction of δ_{CP} for which δ_{CP} can be shown to be non-zero at the 3σ level as a function of $sin^2 2\theta_{13}$. [7] Assumes six years of running by NOvA.

The U.S. groups have also been asked to take responsibility for software management for the Double Chooz project. This includes detector response simulation, neutrino signal and background signal simulation, reconstruction, calibration and analysis. Individuals contributing to the software effort are scattered across the collaboration but the US has until now played a key role in all of these areas, producing the initial version of the codes. The French are providing computing resources, data and software repositories and archiving of documentation at the IN2P3 computing center. While very important to the experiment and the U.S. contribution, there is no capital cost associated with this effort.

1.2 Experimental site: the Chooz nuclear reactors

The antineutrinos used in the experiment are those produced by the pair of reactors located at the Chooz-B nuclear power station operated by the French company Electricité de France (EdF) in partnership with the Belgian utilities Electrabel S.A./N.V. and Société Publique d'Electricité. They are located in the Ardennes region, in the northeast of France, very close to the Belgian border, in a loop of the Meuse river

(see the figure on this proposal's cover). At the Chooz site, there are two nuclear reactors. Both are of the most recent "N4" type (4 steam generators), with a thermal power of 4.27 GW_{th} each, and were recently upgraded from 1.45 GW_e to 1.5 GW_e. Each reactor is off about one month per year. These are pressurized water reactors (PWR) and are fed with UOx type fuel. They are the most powerful reactor type in operation in the world. The first reactor started full-power operation in May 1997, and the second one in September of the same year.

The Double Chooz experiment will employ two almost identical detectors of medium size, each containing 10.3 cubic meters of liquid scintillator target doped with 0.1% of gadolinium. The neutrino laboratory of the first CHOOZ experiment,[1] located 1.05 km from the two cores of the Chooz nuclear plant, will be used again (see Figure 3). This is one advantage of this site compared with other locations. *An even more important advantage is that the major backgrounds at the Far site have all been measured by the original Chooz experiment.* This greatly reduces the scientific risk as compared to sites where backgrounds must be estimated from Monte Carlo simulations.

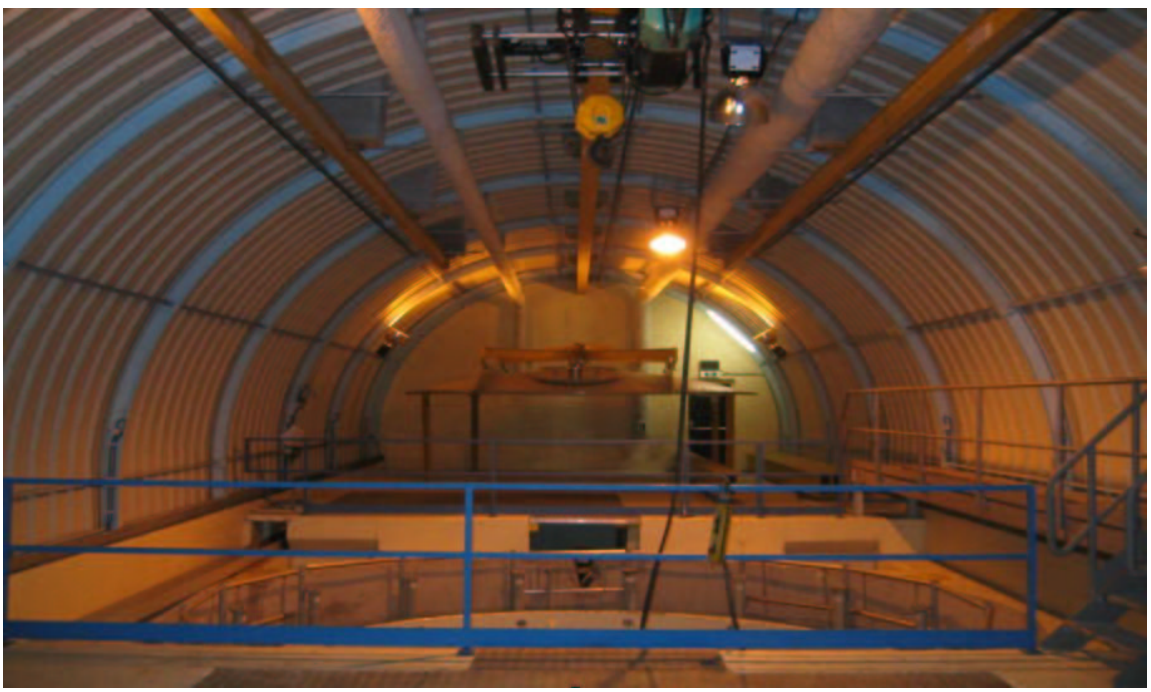

Figure 3: Picture of the Double Chooz-far detector site taken in September 2003. The original CHOOZ laboratory hall constructed by EdF, located close the old Chooz A underground power plant, is still in perfect condition and could be re-used without additional civil engineering construction.

We label this site the far detector site or **Double Chooz-far**. A sketch of the Double Chooz-far detector is shown in Figure 4. The Double Chooz-far site is

[1]For clarity, the first reactor neutrino experiment conducted at the Chooz reactor is herein referred to in uppercase.

shielded by about 300 m.w.e. of 2.8 g/cm^3 rock. It is intended to start taking data at Double Chooz-far at the beginning of 2008.

In order to cancel the systematic errors originating from the nuclear reactors (lack of knowledge of the $\overline{\nu}_e$ flux and spectrum), as well as to reduce the set of systematic errors related to the detector and to the event selection procedure, a second detector will be installed close to the reactor cores. We label this detector site the near site or **Double Chooz-near**.

An initial study has been completed by the French electric power company EdF to determine the best combination of location and overburden as well as the preliminary cost of the needed civil construction. This study suggested the feasibility of excavating a ≈40 m deep shaft at a 250–300 m distance from the nuclear reactor cores. The plan is to start taking data at Double Chooz-near early in 2009.

1.3 Time scale

The schedule for Double Chooz is aggressive in order to take into account the great worldwide interest in θ_{13}. Construction of the far detector will be completed by the end of 2007, and that of the near detector by the end of 2008 (with some uncertainty concerning the schedule of the near laboratory construction). Detector operation will be for 4.5 years, starting with just the far detector, followed by three years of operation with both detectors (2009–2011). Important first results are possible with just the far detector because the luminosity (12 GW-ton-years) of the original CHOOZ experiment will be matched in just a few months. Even with just one detector, Double Chooz will reach a $\sin^2 2\theta_{13}$ sensitivity of 0.06 in 2009, and with two detectors, 0.03 in 2011. Whether running any longer at that time makes sense will depend on an evaluation of systematic errors and backgrounds achieved, as well as the world situation regarding θ_{13}.

1.4 The Collaboration

The Double Chooz experiment is an international collaboration including groups from France, Germany, Japan, the U.S., Spain, Russia, the U.K., Brazil, and Italy. The total number of physicists has grown to well over 100.

The U.S. DOE groups include the University of Alabama, Argonne National Laboratory, the University of California, Davis, Drexel University, the Illinois Institute of Technology, Kansas State University, Lawrence Livermore National Laboratory, Louisiana State University, the University of Notre Dame, Sandia National Laboratory, and the University of Tennessee. The University of Chicago and Columbia University will seek NSF funding for the outer veto system, not described in this document. The calibration, electronics and monitoring systems described in this proposal to the DOE, together with the outer muon tracker system proposal to the NSF, represent a coherent U.S. program to understand backgrounds and systematic errors in the first reactor experiment dedicated to a search for θ_{13}.

Both the U.S. and international groups reflect a great deal of experience with neutrino experiments and with reactor neutrino experiments in particular. Members

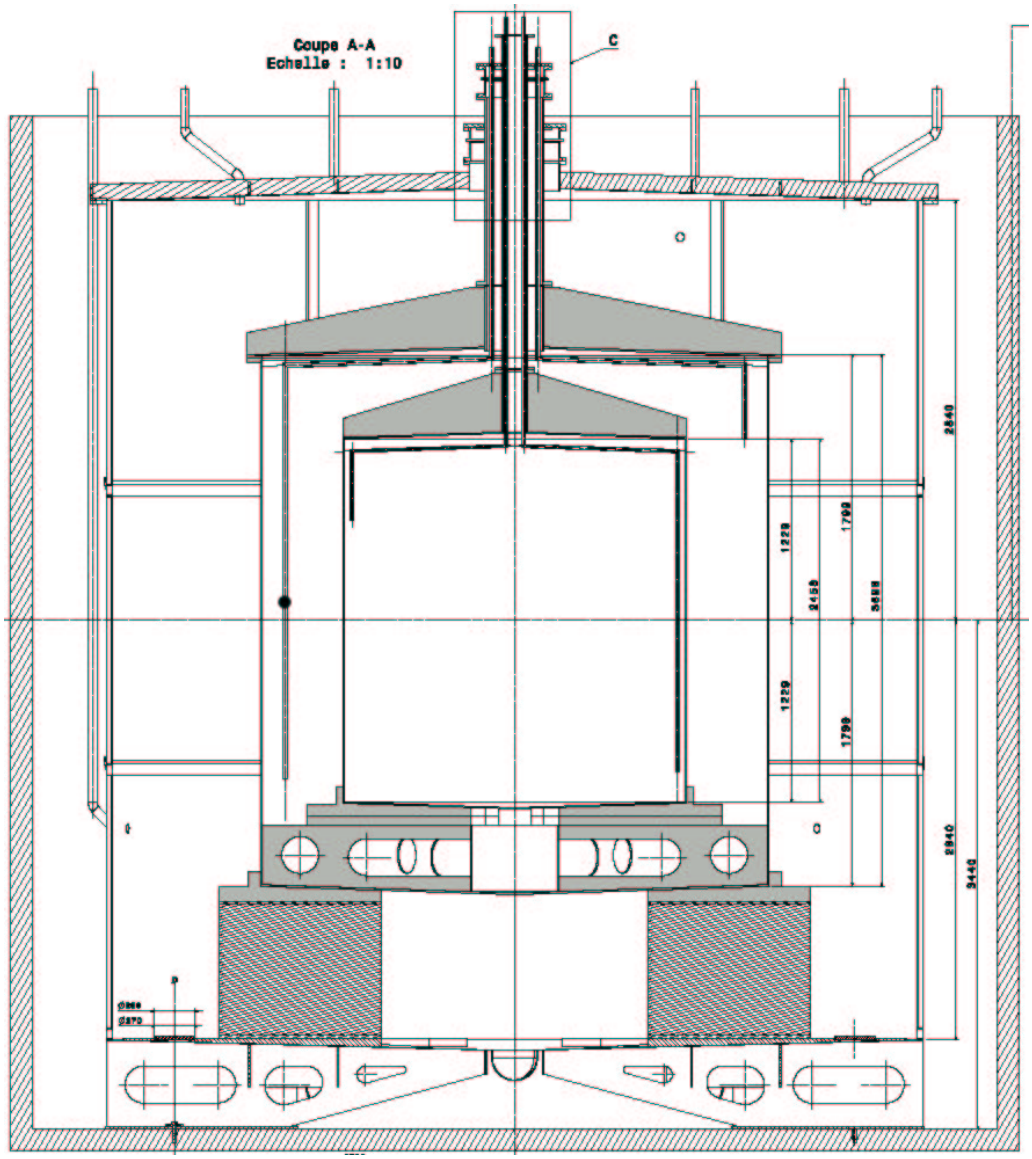

Figure 4: Detail drawing of the Far detector. From the innermost region, one has: the neutrino target, consisting of Gd-doped liquid scintillator enclosed in an 8-mm-thick acrylic vessel; the γ-catcher, undoped liquid scintillator enclosed in a second, 12–15-mm-thick acrylic vessel; the buffer region, nonscintillating oil enclosed in a 3-mm stainless-steel vessel (which also supports the 534 phototubes); the inner veto, scintillating oil enclosed in a 10-mm steel vessel; and 170 mm of steel shielding. (Not shown: steel lid and outer muon veto.)

of the U.S. and French teams were part of the original CHOOZ experiment that gave us our current best limit for θ_{13}. In addition, a substantial number of U.S. members are from the Palo Verde, KamLAND, and San Onofre reactor neutrino experiments. There is also substantial experience from other closely related projects such as SNO, Super-K, MiniBoone, LSND, Minos, NuTeV, Borexino, KASKA, and IMB.

There is a well-established collaboration management team with an active Executive Committee. There are clearly-defined technical working groups and a professional project management team from Saclay and IN2P3. This all works very well. The collaboration has a highly productive environment in which new ideas are welcomed and decisions are based on sound technical evidence via a well-established decision-making procedure. While there is a substantial amount of competition for new ideas, there is also strong mutual support. We believe strongly that the Double Chooz team is the best in the world in this area of physics.

1.5 The Double Chooz Detector Concept

A summary of key detector parameters is given in Table 1. The Double Chooz-far detector will consist of a target cylinder of 115 cm radius and 246 cm height, providing a volume of 10.3 m^3. The near and far detectors will be identical inside the shielding. This will allow a relative normalization systematic error of 0.5%. However, due to the differing overburdens (70–80 vs. 300 m.w.e.), the outer shielding will not be identical, since the cosmic ray background differs considerably between Double Chooz-near and -far. The overburden of the near detector has been chosen in order to keep a high true-neutrino-signal to background ratio.

Starting from the center of the target the detector elements are as follows (see Figure 4):

Target and γ-catcher Target and γ-catcher vessels will be built from acrylic plastic material, transparent to UV and visible photons with wavelengths above 400 nm. The vessels are designed to contain the target and γ-catcher aromatic liquids with long-term hermeticity (no leak for 10 years) and stability. The strongest constraint is the chemical compatibility between the vessel and the scintillating liquids of the target and γ-catcher (chemical stability for a period of at least 5 years). The γ-catcher vessel must also be chemically compatible with the mineral oil of the buffer region, which is however known to be a weaker constraint. Target and γ-catcher vessels will be made of cast acrylic. The target vessel is a cylinder of 246 cm height, 230 cm diameter, and 0.8 cm thickness. It contains a target volume of 10.3 m^3. The γ-catcher is a 55-cm-thick buffer of nonloaded liquid scintillator (22.6 m^3) with the same optical properties (light yield, attenuation length) as the $\overline{\nu}_e$ target. This scintillating buffer around the target is necessary for efficiently measuring the gammas from neutron capture on Gd and from positron annihilation, and to reject the background from fast neutrons.

Nonscintillating buffer A 105-cm-thick region of nonscintillating liquid (114.2 m^3) serves to decrease the level of accidental background (mainly the contribution from photomultiplier-tube radioactivity). This region is crucial to keeping

the singles rate below 10 Hz in the sensitive region (target+γ-catcher). This buffer will reduce the singles rates in each detector by two orders of magnitude with respect to those in CHOOZ, which had no such buffer. The positron detection threshold will be about 500–700 keV, well below the 1.022 MeV physical threshold of the inverse beta decay reaction.

Buffer vessel and PMT support structure This vessel is made of 3-mm-thick stainless steel sheets and stiffeners. A total of 534 phototubes (8 inch) in a uniform array are mounted from the interior surface of the buffer vessel.

Inner veto system A 50-cm-thick veto region filled with liquid scintillator for both the near and far detectors.

Outer veto system An external tracker system will identify and locate "near-miss" muons. This improves the muon rejection by a factor 20 compared to that of the inner veto by itself.

Parameter	Value	Comment
Thermal power	4.27 GW	each of 2 cores
Electric power	1.5 GWe	each of 2 cores
$\overline{\nu}_e$ target volume	10.3 m^3	Gd loaded LS (0.1%)
γ-catcher thickness	55 cm	Gd-free LS
Buffer thickness	105 cm	nonscintillating organic liquid
Total liquid volume	$\sim$237 m^3	
Number of phototubes per detector	534 8"	13% coverage
Far detector distance	1050 m	averaged
Near detector distance	280 m	averaged
Far detector overburden	300 m.w.e.	hill topology
Near detector overburden	70–80 m.w.e.	shaft
Relative systematic error	0.5%	
Effective bin-to-bin error	1%	background systematics
Running time with far detector only	1–1.5 year	
Running time with far+near detector	3 years	
$\sin^2(2\theta)$ goal in 3 years	0.02–0.03	(90% CL)

Table 1: Key parameters of the proposed Double Chooz experiment.

1.6 Physics Reach

1.6.1 Signal

In this section we provide a short summary of the antineutrino signal expected in the Double Chooz detectors. A detailed summary of the calculated spectra and rates can be found in Full Collaboration Double Chooz Proposal [1].

The antineutrino flux provided by the two nuclear cores of the Chooz power plant results from β^- decay of the fission products of four main isotopes ^{235}U, ^{239}Pu,

^{241}Pu and ^{238}U. The overall $\bar{\nu}_e$ spectrum is evaluated from measurements of ^{235}U, ^{239}Pu, ^{241}Pu and theoretical prediction for ^{238}U [14]. We take an average burning cycle composition of 55.6% of ^{235}U, 32.6% of ^{239}Pu, 7.1% of ^{238}U and 4.7% of ^{241}Pu. However, a ten percent burnup effect is taken into account in detailed simulations.

The maximum operating thermal power of each core amounts to 4.27 GW. We denote the west and east reactor cores by R_W and R_E, respectively. The far detector is located at a distance of $1,114.6 \pm 0.1$ m from R_E, and at 997.9 ± 0.1 m from R_W, leading to 2.86 neutrino events per hour. A near detector preferred location is foreseen at 290.7 m from R_E and 260.3 m from R_W, leading to 42 events/h. At this location, both detectors receive the same neutrino flux ratio coming from both nuclear cores. This cancels systematic uncertainties related to the uncorrelated fluctuations of the thermal power of each reactor.

Each of the Double Chooz target volumes contains 10.32 m^3 of liquid scintillator (see Section 1.7.3). Neglecting the small amount of fluors as well as the gadolinium compound, the scintillator can be described as 20% PXE ($C_{16}H_{18}$) and 80% dodecane ($C_{12}H_{24}$). This leads to 6.79×10^{29} free protons available for the inverse β-decay detection reaction:

$$\bar{\nu}_e + p \rightarrow e^+ + n. \tag{1}$$

The global load factor of the Chooz power plant was 73.3% and 81% for R_W (Chooz–B1), and 79.7% and 76.2% for R_E (Chooz–B2) in 2003 and 2004, respectively. Assuming an averaged value of 78%, then after 5 years the amount of data available would be $76,000$ reactor neutrino events in the far detector and $800,000$ events in the near detector, accounting for the reactor duty cycle and all estimated detector efficiencies. Neutrino rates and associated information are summarized in Table 2.

	Near detector	Far detector
Distance from West reactor (m)	290.7	$1,114.6 \pm 0.1$
Distance from East reactor (m)	260.3	998.1 ± 0.1
Detector efficiency	80%	80%
Dead-time efficiency	70%	97%
Reactor efficiency	78%	78%
Rate without efficiency (d^{-1})	1012	68.8
Rate w. detector & dead-time efficiency (d^{-1})	566	53.4
Integrated rate (y^{-1})	$161,260$	$15,200$

Table 2: Neutrino-induced event rates expected in the near and far detectors, with and without reactor and detector efficiencies. Final distances for the near detector have not been decided yet, but the values presented are good estimates within 30%. The rate without efficiency is used for signal to background comparison. The integrated rate in the last line includes detector efficiency, dead time, and reactor off periods averaged over a year. Distances are horizontal displacements, but rates include the effects of detector elevation.

1.6.2 Experimental errors

Double Chooz will use two $\overline{\nu}_e$ detectors in order to cancel or decrease significantly the systematic uncertainties that would limit the sensitivity to θ_{13}. For the sake of comparison, the total systematic error of the CHOOZ experiment amounted to 2.7% [15]. This error was dominated by the reactor antineutrinos flux and spectrum uncertainties, that amounted to 1.9%. At neutrino luminosities addressed by Double Chooz the relative normalization between the two detectors is the most important source of error and must be carefully controlled. The goal of Double Chooz is to reduce this uncertainty to 0.5%. Systematic errors include those associated with the reactor and with the detector. Since the neutrino flux is isotropic, all the reactor induced systematic uncertainties cancel but the solid angle, which is less than 0.1%.

Improvements in the detector design between CHOOZ and Double Chooz will lead to a reduction by a factor of three in the uncertainties related to the detector. A shield will be used instead of the sand that was used in the CHOOZ experiment. A non scintillating region, called the "buffer", will be created to reduce the single rate in the target+γ- catcher. An efficient inner veto is designed for muon tagging and fast neutron background rejection. An outer muon tracker will allow us to further reduce the cosmogenic backgrounds. The concentration of Gd will be identical in both detectors since target liquids will be produced in a single batch. A neutrino event is defined by the neutron capture on Gd after positron annihilation. It is possible to have a neutrino interacting in the target region but a neutron capture in the γ-catcher region, which we call "spill out". It is also possible to have a neutrino reaction in the γ-catcher region and an n capture on Gd in the target region, which we call "spill in". These tend to offset each other, but the cancellation is not exact. In CHOOZ the spill-in effect accounted for 4% of the events, and the spill-out 2% (the quoted error was about 40%). It led to a $\sim$1% uncertainty (from Monte-Carlo simulation) on the final result. However, the effect cancels if the two detector have a similar target (a few millimeter geometrical effect has a negligible effect on the results). Nevertheless, we plan to place neutron sources in the γ-catcher and target regions near to directly measure these effects. The target liquid will be prepared in a large single batch of about 20 tons. Thus, the uncertainty on the scintillator density ($\sim$0.01%) as well as chemical composition ($\sim$1%) makes a negligible contribution to the relative normalization error.

$\overline{\nu}_e$ events manifest themselves as two local energy depositions of more than 1 MeV in less than 100 μs. The second energy deposition (delayed energy) should be consistent with neutron capture on Gd, roughly $8 \pm 2\ MeV$. In the CHOOZ experiment, the selection cut uncertainty was 1.5%, coming from a set of seven analysis cuts used to extract the $\overline{\nu}_e$ candidates [15]. The Double Chooz non-scintillating buffer allows us to reduce the number of selection cuts, while keeping only a small accidental background contamination (a few percent of the signal).

The positron induced by the antineutrino interaction in the target has a very short track in the detector. It annihilates and creates two back-to-back 511 keV gammas. One or both of the gammas may leave the target, but most of the time they will deposit their energy in the target+γ-catcher sensitive volume. Thanks to

	Single Detector	Double Chooz
Volume	0.2%	0.2%
Ratio H/C	$< 0.5\%$	negligible
Density	0.01%	negligible
Gravimetry (g)	0.005%	0.002%
Total	<0.55%	0.2%

Table 3: Systematic uncertainties related to the target free proton measurement. In Double Chooz the systematics associated to the number of target protons will be 0.2% since a single batch will be prepared for both detector target. The "Single Detector" case is very important for the non proliferation branch of Double Chooz, however, so we will make an effort for an accurate determination of this parameter. The H/C determination depends on the scintillator solvent composition. Dodecane is favored over mineral oil whose composition is less well defined (1%). In the former case we estimate a systematic error contribution of <0.55%.

the addition of a buffer volume between phototubes and the active detector region, the energy threshold will be around 700 keV. Using the expected energy resolution of 7% at 1 MeV, the fraction of neutrino events leading to a positron below the threshold will be negligible.

Neutrons induced by neutrino interactions can travel about 5 cm before being captured. The thermal neutron is captured either on hydrogen or on gadolinium (neglecting carbon captures for the moment). In some cases the gammas emitted after the capture on Gd can escape the target+γ-catcher volume. Making an energy cut on the delayed neutron energy at 6 MeV will then result in an uncertainty related to the uncertainty in energy scale between the near and far detectors. An uncorrelated uncertainty of 100 keV in the energy scale leads to a 0.2% uncertainty in the neutron selection. Table 4 summarizes the identified systematic errors that are currently being considered for the Double Chooz experiment. A full description of these estimates can be found in the Full Double Chooz Collaboration Proposal [1].

1.6.3 Backgrounds

In Double Chooz there will be backgrounds from primordial and man-made radioactivity, as well as backgrounds induced by cosmic ray interactions. Here we consider backgrounds from a number of sources. Since the reactor neutrino signature involves a coincidence, more than one source of background may be considered at the same time.

One very important advantage of the Double Chooz far site is that the important backgrounds have already been measured there directly by the original Chooz experiment. This means that we need not rely on computer simulations to estimate the effects of such backgrounds on our sensitivity. In the background calculations below

		CHOOZ	Double Chooz
Reactor Solid Angle		—	0.06%
Free H in target	Volume	0.3%	0.2%
	Fiducial Volume	0.2%	negligible
	Density		negligible
	H/C	0.8%	negligible
Electronics	Dead Time	—	negligible
Positron	Escape	0.1%	negligible
	Energy Cut	0.8%	negligible
Neutron	Escape	1.0%	negligible
	Capture (% Gd)	0.85%	0.3%
	Energy Cut	0.4%	0.2%
Antineutrino Coincidence	Time Cut	0.4%	0.1%
	Distance Cut	0.3%	not used
	Single neutron	0.5%	not used
Total		1.5%	0.5%

Table 4: Comparison of systematic errors in CHOOZ and Double Chooz

we have used the measured values at Chooz for the rate of neutron-like events and also for the production of 9-Li. It is worth noting that in the case of the former, the measured value is almost an order of magnitude higher than the calculated one - demonstrating the power of having data rather than a Monte Carlo in designing the detector and calculating the sensitivity.

1. **Accidentals from natural radioactivity**

   Naturally occurring radioactivity can create accidental as well as correlated backgrounds. Gamma, beta and neutron signals in the detector or in the surrounding rock may generate accidental background events which mimic the prompt (positron-like) $\overline{\nu}_e$ interaction signal. Delayed background (neutron-like) events can come from actual neutron capture on Gd. However, some neutron-like events could also be generated by bremsstrahlung photons radiated from cosmic muons which traverse the rock surrounding the detector. The total neutron like background rate was measured at the far site by the CHOOZ detector. The rate was found to be $45 \pm 2/h$ (after cuts) [15]. This high rate was never explained by the CHOOZ experiment, and our current simulation is not reliable in that it gives a much smaller rate. *We therefore use the measured CHOOZ rate for all the calculations that follow.*

   Based on that *measurement* (rather than a calculation) we assume a neutron rate of 83/h ($2.3 \cdot 10^{-2} Hz$) for Double Chooz at the far site. Conservatively assuming this scales like the muon rate (since we don't know the mechanism in order to determine the scaling with mean energy) would give 913/h at the near detector. Note that this rate is not a relevant contribution to the rate of

positron-like events. For example, the phototubes are expected to contribute to the rate of positron-like single events at the level of a few events per second.

The accidental background rate b_{acc} is given by $b_{acc} = b_p V_p b_d V_d \tau_d$. Here b_p and b_d are the specific background rates (in units of $Hz\, m^{-3}$) for the prompt and the delayed events, respectively. The time window for the coincidence is given by $\tau_d = 100\ \mu sec$, where $V_p = V_T + V_{GC} = 32.89\ m^3$ is the relevant volume for positron-like events (no use of the distance cut), and $V_d = V_T = 10.32\ m^3$ is the relevant volume for the neutron-like events. Thus $R_p = b_p V_p$ is the rate of prompt positron-like events, and $R_p = b_d V_d$ is the rate of delayed neutron-like events. A good estimation of the daily accidental background without distance cut is given by

$$b_{acc} = 0.2 \times \frac{R_p}{1\ s^{-1}} \times \frac{R_d}{83\ h^{-1}}\ day^{-1}\ . \tag{2}$$

This rate can easily be measured to better than 1% by independently measuring the singles rates for electron-like and neutron-like events. Thus we can conservatively require that the accidental background rate from all materials be less than 3% of the neutrino signal (69/d and 1012/d at the far and near site respectively), we get the constraints $R_p^{far} < 10$ Hz and $R_p^{near} < 14$ Hz, about the same for each.

Selection of high purity materials for detector construction and passive shielding provide an effective countermeasure against accidental background events. See section 5 for a complete discussion of radiopurity of materials. A major contributor to the singles rates for gammas is expected to be the photomultiplier tubes, mainly due to impurities in the glass. Thanks to the oil buffer, this is expected to be at the level of a few Hertz. Several phototube candidates from ETL, Hamamatsu and Photonis are under investigation. Results are summarized in section 5 and discussed in detail in the Full Collaboration Double Chooz Proposal reference [1]. Estimates can be given taking into account the range of measurements for these phototube candidates. From these measurements and those done for other common detector materials from KamLAND and SNO, the expected singles rate (positron-like) above 700 keV is expected to be below 10 Hz, which is sufficient for our purposes. Note that making sure that we are within this specification is a major part of the proposed scope of this proposal.

2. **Muon rates**

To properly simulate the detector response to cosmic muons, it is necessary to use angular resolved muon distributions and energy spectra for both detector locations. The muon propagation tool MUSIC [16] was used for this purpose, in combination with GEANT4- and FLUKA-based simulations.

A measurement of the angular distribution of muons at the Double Chooz far site was performed prior to the CHOOZ experiment [17]. A modification of the MUSIC code was used to create an independent spectrum and angular distribution by propagating surface muons through rock [18]. Details on the rock

composition, as measured by chemical analysis of several samples in [17], were taken into account. The simulation predicts a muon flux of $6.2 \cdot 10^{-5} cm^{-2} s^{-1}$ (about 5 Hz through the target region), slightly higher than the measured value quoted in [15]. For the near detector the calculated rate is $5.9 \cdot 10^{-4} cm^{-2} s^{-1}$ (about 55 Hz through the target). The mean muon energy at the far (near) detector location will be about 61 GeV (30 GeV). With these muon distributions, a secondary neutron spectrum was generated with the DCGLG4sim software, which was used as a starting point for fast neutron simulations.

3. **Bremsstrahlung photons**

   All energy deposits over 6 MeV isolated in time from other deposits are candidate single neutrons. In the first CHOOZ experiment, such events occurred with a rate of about $2 \cdot 10^{-2}$ Hz. The origin of these energy deposits is unknown. The radial distribution of the reconstructed vertices, decreasing by two orders of magnitude from the outer wall to the center, suggests an origin outside the detector. The hypothesis has been made that neutron-like events could be due to bremsstrahlung photons radiated from cosmic muons which traverse the rock surrounding the detector ("near-miss" muons). A detailed Monte Carlo study was carried out to test this hypothesis. Cosmic muon samples were generated according to the measured angular distributions [17] at the site and an energy spectrum appropriate for an overburden of 300 m.w.e. [19]. The interactions with the rock and in a detector with similar geometry to CHOOZ were simulated with the GEANT4 package. Simulation of photons from "near-miss" muons explains only 1/10 of the neutron-like energy deposits observed in CHOOZ. Thus in calculating the rate of coincidences we use the higher measured rather rather than the lower calculated one. Note that this refers to the rate of *neutron capture-like* events. The calculated rate of *fast neutrons* agrees reasonably well with simulations.

4. **Fast neutron background**

   Fast neutrons were the single main source of background in the CHOOZ experiment [15]. These neutrons are created by "near-miss" muons interacting in the material surrounding the detector. Their long mean free path allows them to traverse the entire detector. Some of them slow down in the detector material and are captured in the target. The recoil proton can mimic the positron (the deposited energy is higher, but part of it can be unseen), and is correlated with the subsequent neutron capture, similar to a real correlated neutrino event. Other particles created by neutron interactions in the target can also contribute. The energy spectrum of these events is known from previous experiments to be very smooth. In the CHOOZ paper (Figure 46 of [15]) a rather flat spectrum is shown, with some saturation effect causing a slow rise toward low energy. Since there are no reactor neutrinos beyond about 15 MeV, this background can be monitored in the 15 – 50 MeV range. The total correlated background in the CHOOZ experiment was published at 1.01 event/day, and found to be in good agreement with the extrapolation of the

Event/day	Simulation		Data
	Mean	90% C.L. Upper Limit	
CHOOZ	0.8	3.0	$1.01 \pm 0.04 \pm 0.1$
Double Chooz far	0.2	0.8	—
Double Chooz near	1.3	5.0	—

Table 5: Summary of fast neutron background predictions in Double Chooz near and far detectors. This can be compared with the data of the CHOOZ experiment at the far site as well as its new simulation.

measured rate over 15 MeV. Our new simulation [29] obtained a mean value of 0.8 events/day (less than 3.0 events/day at 90% confidence level). This is in good agreement with the 1 event/day quoted in [15]. The same simulation obtained 0.2 event/day at the Double Chooz far site and 1.3 event/day at the near detector. This is significantly less than in the CHOOZ experiment, as expected due to improvements in the detector design. Using steel instead of sand increases the neutron path toward the target by about one attenuation length, from which a factor 3 decrease can be predicted. This work was done without using the muon tracker; an additional background rejection by a factor of 15 thus is expected, making this fast neutron background very small.

Another handle for rejecting fast neutrons is that some would make an energy deposit in the inner veto. In the Double Chooz experiment, some pulse shape discrimination (PSD) will be possible, allowing us to separate the recoil proton signal, which is more highly ionizing and slower, from that of the neutrino. This will be used not to reject events (which would create systematic errors), but to tag and monitor the background, and measure its energy shape. Since it will also be measured above 15 MeV and below 1 MeV (once the accidentals events are subtracted), a three-component fit will be possible. A summary of fast neutron backgrounds is given in Table 5.

	Steel shielding	Buffer structure	Buffer oil	Chimney	Target structure
mass (tons)	14	7	4	0.005	0.1
Capture rate	70/s	40/s	0.5/s	$0.6\,10^{-3}$/s	0.01/s
neutron rate	80/s	50/s	0.8/s	10^{-3}/s	0.015/s
target rate (no Veto)	1/d	5/d	160/d	0.1/d	100/d
target rate (Veto)	0.05/d	0.005/d	0.16/d	0.1/d	0.1/d

Table 6: Fast neutron production rate from muon capture in the near detector (overburden 80 m.w.e). Rates were calculated for a volume of material within one interaction length of each component. Rates are for the production of single events under the assumption that the muon tagging efficiency of the two veto systems plus detector is only 99.9%.

5. **Muon capture**

   Muon capture contributes to the background by creating gammas, neutrons, and cosmogenic nuclei. Cosmogenic nuclei are described on page 23 and gamma backgrounds have been discussed previously in this section. We focus here on neutrons from such a capture in the near detector. These neutrons are a potential source of correlated background: they may propagate though the detector and reach the γ-catcher or target, creating recoil protons that can mimic the inverse beta decay positron signal, and subsequent capture on Gd. Of course, there will be two independent muon veto systems with a combined efficiency estimated to be better than 99.9%, and in general there is little chance for a muon to enter the central regions of the detector without depositing a truly huge amount of light that could also be used to veto these events. Nevertheless, we have performed simulations of this background under the conservative assumption that the overall efficiency of the vetoes+detector is only 99.9%. For muons that stop in the shield, a 95% efficiency has been used since the muons do not penetrate the inner veto. The rate of neutrons entering the target from various detector regions is shown in Table 6.

   These rate estimates could vary as much as an order of magnitude, but it's clear that not every such neutron will make a correlated event. Nevertheless, we have conservatively taken these rates to be the expected number of events from muon capture in our sensitivity estimates.

6. **Cosmogenic correlated background: lithium-9**

   The cosmogenically produced isotope ^{9}Li is considered the most serious problem for reactor experiments, since its beta decay has a branching ratio of about 50% into states that de-excite via neutron emission, and the resulting electron plus neutron combination can mimic a reactor neutrino signal. The 178 ms half life could also make it difficult to veto since it would lead to an unacceptable deadtime. In addition, the best measurements of cosmogenic production come

from large depths, where the hard muon flux makes extrapolation to shallow depths uncertain. Therefore we discuss this background here in some detail.

We have the great advantage of having the data from the original CHOOZ experiment to draw on (especially 138 days of reactor off data). This allows us to extract the expected rate of ^{9}Li at our far laboratory based on data rather than MC or extrapolation from large depths. The expected rate is 1-2% of the signal (before veto). Thus, this is a background we can handle by veto and measurement, as shown below.

For the KamLAND experiment, it was found that a cut of 10^6 photoelectrons was effective in tagging muon-initiated showers that were important in ^{9}Li production. The 10^6 photoelectron cut in KamLAND has been simulated using the KamLAND detector simulation program, KLG4sim. The simulation predicts that about $(7.7 \pm 0.4\%)$ of cosmic ray muons will be eliminated by a cut at 10^6 p.e. (which corresponds to roughly 3.3 GeV of deposited energy). This is to be compared with 6% obtained by an analysis of one day of KamLAND data — a reasonably good agreement. The *same* simulation package adapted for Double Chooz depth (300 m.w.e.) and geometry predicts that a similar cut (slightly above the peak of the energy loss distribution, about 2.8 GeV) would eliminate only 1.3% in Double Chooz (Far). With a muon rate (through the whole detector, not just the target) of $\approx$ 25 Hz, this would correspond to a veto rate of only one every 3 seconds. Thus extrapolation of the KamLAND measurement would give a rate in the far detector that could be vetoed.

We have extracted the ^{9}Li production rate in the CHOOZ experiment in three different ways: (1) total background rate, (2) spectral fit to official CHOOZ data between 2.8 and 10.0 MeV, and (3) a more recent spectral fit to extended CHOOZ data between 2.8 and 30.0 MeV. CHOOZ had a measured accidental coincidence background of 0.42 ± 0.05 event/day and a background from fast neutrons of 1.01 ± 0.11 event/day during the period when most of their reactor-on data were taken. The corresponding background rate from reactor-off data in this same period was 1.4 ± 0.24 event/day, which is consistent with the sum of the two individual rates. Based on the 0.11 event/day uncertainty in extrapolating the proton recoil spectrum below 10 MeV, there could be as much as 0.2 event/day of ^{9}Li hidden under the reactor signal. This analysis depends critically on systematic uncertainties which are difficult to quantify. A better technique is to fit the shape of the prompt energy spectrum. A spectral fit to the official CHOOZ reactor-off data showed a flat proton recoil visible energy spectrum. The fit used a ^{9}Li-shaped decay spectrum that includes the effect of the broad lines on the endpoint. The fit is only done above 2.8 MeV to avoid the peak due to accidental coincidences below that energy. The best fit for the ^{9}Li rate is 0.6 ± 0.4 event/day, although in this fit the two backgrounds are highly correlated. The correlation between the two backgrounds can be broken by fitting the background above 10 MeV, beyond the ^{9}Li endpoint. Such data are shown in Figure 5. Now the correlation is almost completely broken, and the measured rate is 0.7 ± 0.2 event/day.

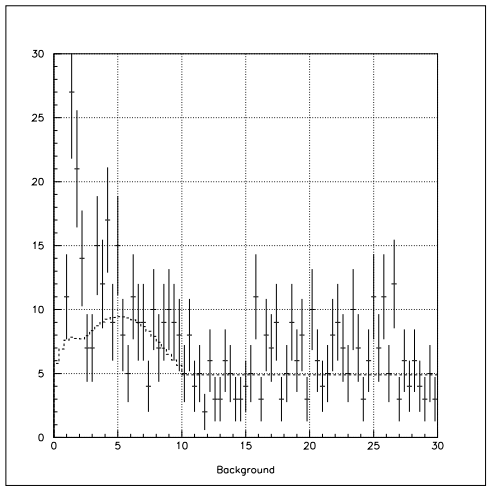

Figure 5: Unofficial CHOOZ Reactor Off visible energy spectrum fit with a combination of flat and ^{9}Li-shaped background. The fit is only above 2.8 MeV to avoid the accidentals below that energy. The best fit for ^{9}Li is 0.7 ± 0.2 event/day.

The three methods using CHOOZ data imply a ^{9}Li rate for Double Chooz in the range 0.5 to 1.5 event/day, or about 1-2% of the expected signal. This is a rate that can be handled either by veto, measurement to an accuracy of 10%, or (most likely) both. With the expected muon rate through the detector of 25 Hz, we could afford to veto these muons for up to 400 ms (factor of ten reduction) before incurring substantial dead time. Thus ^{9}Li in the Far Detector can be dealt with in multiple ways. In the near Detector, the extrapolated rate using an $E^{0.75}$ dependence gives a rate of 9/day, or 0.9% of the expected signal. The muon rates are expected to be too high to effectively veto ^{9}Li, however, a 17% measurement of this rate could be done with the expected "one-reactor-off" time required for refueling (one month per year per reactor) over five years. With only two weeks of "two-reactor-off" time a 9% measurement could be made. Thus, this background can be subtracted to a precision of at least 0.15% and most likely better if a small amount of time is available with both reactors off. *Note: with more than two cores "All Reactors Off" time is likely to never occur - another advantage of the Chooz site.*

A summary of backgrounds estimated in Double Chooz is presented in Table 7.

1.6.4 Sensitivity

Figure 6 shows the positron energy spectra expected at the near and far detectors of Double Chooz for 3 years of data taking, assuming a true value of $\sin^2 2\theta_{13} = 0.1$ and $\Delta m^2_{31} = 2.5 \times 10^{-3}$ eV^2. The sensitivity and discovery potential of Double Chooz are given in Table 9. Systematic error parameters and values are listed in Table 8 as described in Section 2.4 of the Full Collaboration Double Chooz Proposal. The θ_{13} sensitivity contour together with a recent global analysis is shown in Figure 7, while the Double Chooz sensitivity as a function of time is given in Figure 8.

Detector	Site		Background				
			Accidental		Correlated		
			Materials	PMTs	Fast n	μ-Capture	^{9}Li
CHOOZ		Rate (d^{-1})	—	—	—	—	0.6 ± 0.4
(24 ν/d)		Rate (d^{-1})	0.42 ± 0.05		1.01 ± 0.04(stat) $\pm$ 0.1(syst)		
	Far	bkg/ν	1.6%		4%		
		systematics	0.2%		0.4%		
Double Chooz		Rate (d^{-1})	0.5 ± 0.3	1.5 ± 0.8	0.2 ± 0.2	< 0.1	1.4 ± 0.5
(69 ν/d)	Far	bkg/ν	0.7%	2.2%	0.2%	<0.1%	1.4%
		systematics	<0.1%	<0.1%	0.2%	<0.1%	0.7%
Double Chooz		Rate (d^{-1})	5 ± 3	17 ± 9	1.3 ± 1.3	0.4	9 ± 5
(1012 ν/d)	Near	bkg/ν	0.5%	1.7%	0.13%	<0.1%	0.9%
		systematics	<0.1%	<0.1%	<0.1%	<0.1%	0.5%

Table 7: Summary of the background subtraction error at the far and near detectors. Background rates and shapes with their corresponding uncertainties are used. For 9-Li, the fact that we can measure the rate with reactor off data is not used in calculating the systematic error, which will further lower the uncertainty.

Error type	k	$c^D_{i,k}$	$\alpha^D_{i,k}$	$S^D_{i,k}$	σ^D_k
Global normalization	1	$1/2N_{\text{bins}}$	α_{abs}	T^D_i	$\sigma_{\text{abs}} = 2.0\%$
Relative normalization	2	$1/N_{\text{bins}}$	α^D_{rel}	T^D_i	$\sigma_{\text{rel}} = 0.6\%$
Spectrum shape	3	$1/2$	$\alpha_{i,\text{shp}}$	T^D_i	$\sigma_{\text{shp}} = 2.0\%$
Energy scale	4	$1/N_{\text{bins}}$	$\alpha^D_{i,\text{scl}}$	$\left.\frac{\mathrm{d}N^D_i}{\mathrm{d}\alpha_{i,\text{scl}}}\right\|_{\alpha^D_{i,\text{scl}}=0}$	$\sigma_{\text{scl}} = 0.5\%$
Δm^2_{31} knowledge	5	$1/2N_{\text{bins}}$	$\alpha_{\Delta m^2_{31}}$	—	$\sigma_{\Delta m^2_{31}} = 10 - 20\%$

Table 8: Table of systematic parameters used in Double Chooz. See the Full Double Chooz Collaboration Proposal [1] for a complete description of these parameters.

1.7 Detector Structures and Materials

1.7.1 Detector dimensions

A full description of the Double Chooz detector can be found in Chapter 3 of the Full Collaboration Double Chooz Proposal [1]. Detector dimensions are summarized in Tables 10 and 11.

Target and γ-catcher vessels will be built from acrylic plastic material, transparent to photons with wavelengths above 400 nm. The vessels are designed to contain

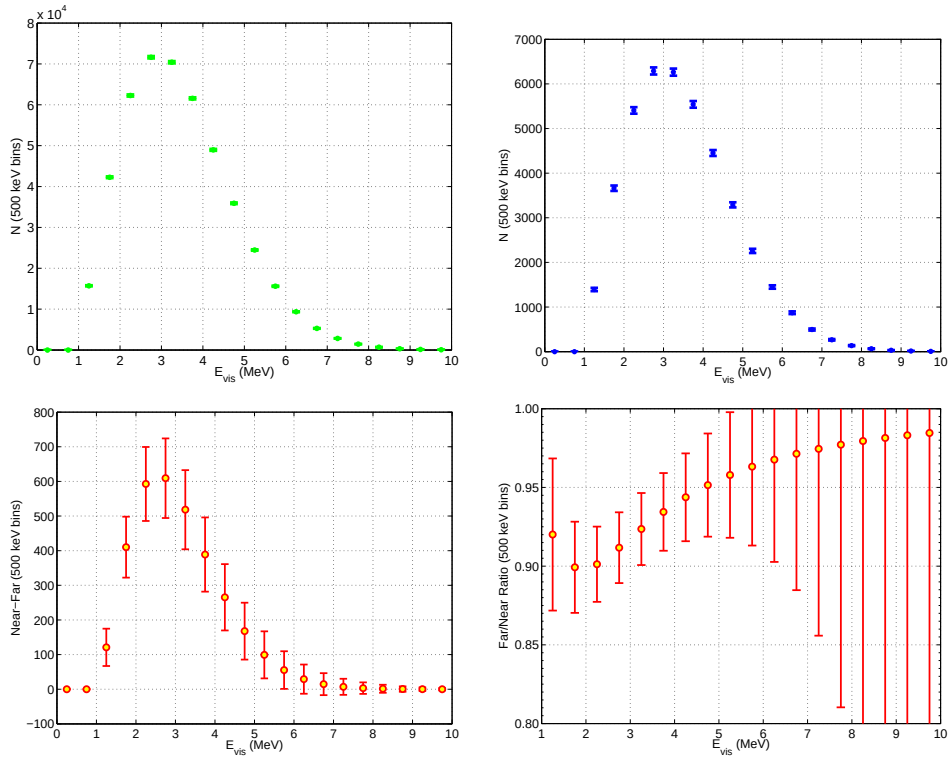

Figure 6: Expected signal assuming a true value of $\sin^2 2\theta_{13} = 0.1$ and $\Delta m^2_{31} = 2.5 \times 10^{-3}$ eV^2, for 3 years of data taking with both detectors. Top left: positron energy spectrum at the near detector. Top right: positron energy spectrum at the far detector. Bottom left: spectrum difference between the near and far detectors (normalized to the far detector statistics). Bottom right: far to near spectrum ratio. Errors bars shown are statistical only.

the target and γ-catcher aromatic liquids with long-term hermeticity (no leak for 10 years) and stability. The strongest constraint is that of chemical compatibility between the vessel and the scintillating liquids of the target and γ-catcher: For a period of at least 5 years, we can tolerate neither a change in properties (scintillation and absorbency) of the liquids nor a degradation of the acrylic material (cracking or crazing of more than a few percent of its surface area). The γ-catcher vessel must also be chemically compatible with the mineral oil of the buffer region; this is known to be a weaker constraint.

A stainless steel buffer vessel encloses the γ-catcher and target. The buffer vessel is a cylinder of 5680 mm height, 5522 mm diameter (external dimensions), and 3 mm thickness. It weights 7.7 tons and contains a volume of 114.2 m^3 (without the chimney).

1.7.2 PMT support structure

Each photomultiplier will have an independent mechanical support. We are planning to use lightweight mounts similar to those developed for the MiniBooNE experiment.

Δm^2_{31} (10^{-3} eV^2)	1.8	2.0	2.2	2.4	2.6	2.8	3.0	3.2	3.4
Sensitivity (90% C.L.)	0.043	0.037	0.032	0.030	0.027	0.025	0.024	0.023	0.022
Discovery potential (3σ)	0.078	0.067	0.060	0.054	0.05	0.046	0.044	0.042	0.041

Table 9: Sensitivity and discovery potential dependence on Δm^2_{31}, for 3 years of data taking with both detectors.

Inner Detector	Inner Diameter (mm)	Inner Height (mm)	Thickness (mm)	Filled with	Volume (m^3)	Mass (tons)
target	2300	2458	8	Gd-LS	10.3	0.35
γ-catcher	3392	3574	12(-15)	LS	22.6	1.1–1.4
PMTs	—	—	—	—	—	—
buffer	5516	5674	3	Oil	114.2	7.7
veto	6590	6640±100	10	Oil	90	20
shielding	6610	6660±100	170	Steel	—	300
pit	6950	7000	—	—	—	—

Table 10: Dimensions of the mechanical structure of the detector.

These supports are made from stainless-steel wire of 2.5 mm diameter (see Figure 9). The inner face of the buffer vessel will hold each phototube support in its assigned location. These locations will be defined by ribs welded to the buffer-vessel inner wall during the assembly process. The photomultiplier supports will be bolted to the ribs, and the photomultiplier locations will be surveyed after mounting.

The detector outer vessel will be a steel tank surrounding the veto region, 500–600 mm away from the buffer vessel. It is a cylinder of 6966 mm height, 6966 mm diameter (external dimensions), and 10 mm thickness, weighing 20 tons. This tank will contain all other liquids in case of any internal mechanical failure. It will be closed by a top lid coupled with a nitrogen-blanket system to prevent oxygen contamination of the liquids. Outside this vessel a 170 mm thickness of low-activity steel shielding will protect the detector from the natural radioactivity of the rock around the pit.

1.7.3 Scintillator and Buffer Liquid

In the Double Chooz detector design there are three separated volumes filled with liquids inside the stainless steel buffer tank. The inner volume is the $\overline{\nu}_e$ target and it will contain 10.3 m^3 of liquid scintillator loaded with gadolinium (Gd-LS) at a concentration of approximately 1 g/ℓ. The acrylic vessel holding the target volume is surrounded by the γ-catcher with a volume of 21.5 m^3. This volume is filled with a

Region	target	γ-catcher	buffer	veto
Radial Thickness (mm)	1150	550	1050	500
Vertical Thickness (mm)	2458	550	1050	500 below and 600 above

Table 11: Thickness of the four detector regions filled with liquids

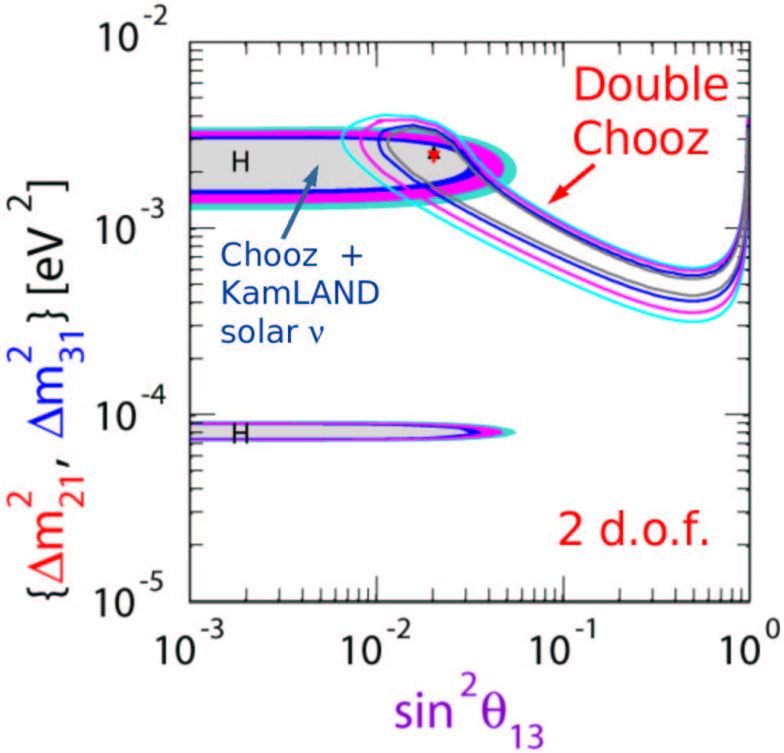

Figure 7: Double Chooz sensitivity contours (gray $1\,\sigma$, blue 90%, magenta $2\,\sigma$, cyan $3\,\sigma$ C.L.) in $(\sin^2\theta_{13}, \Delta m^2_{31})$ plane generated for $\sin^2\theta_{13} = 0.02$ and $\Delta m^2_{31} = 2.5 \times 10^{-3}$ eV^2 (which is also the best fit) with 1% background in near and far detectors, systematics included as summarized in Table 8 and parametrization described in reference [1], except that we have relaxed the constraint on Δm^2_{31} and computed contours with 2 degrees of freedom assuming 3 years of data taking. Also shown here, the current contours from global analysis with the same color convention [20]. Double Chooz is able to provide a 20% precision measurement of θ_{13} as long as this parameter is not too low.

Gd-free scintillator. Finally, there is a volume of about 100 m^3 outside the γ-catcher containing a non-scintillating buffer liquid. On the inner wall of this volume the PMTs will be mounted. The densities of the liquids should be similar in all of the three volumes in order to avoid strong buoyancy forces in the detector.

The Gd-loaded scintillator for the targets of both detectors will be produced together as a single batch to assure identical proton per volume concentrations in both detectors, and to assure that if there are any aging effects, they are more likely to be the same for both detectors. As scintillator solvent it is planned to use a PXE (phenyl-xylylethane)/dodecane mixture at a volume ratio of 20:80. The admixture of the dodecane reduces the light yield, but it improves the chemical compatibility with the acrylic and increases the number of free protons in the target. In addition to these technical requirements, there are safety considerations to be taken into account in the choice of the solvent mixture. In particular, both components have high flash points (PXE: fp 145°C, dodecane: fp 74°C). The scintillation yield of the unloaded

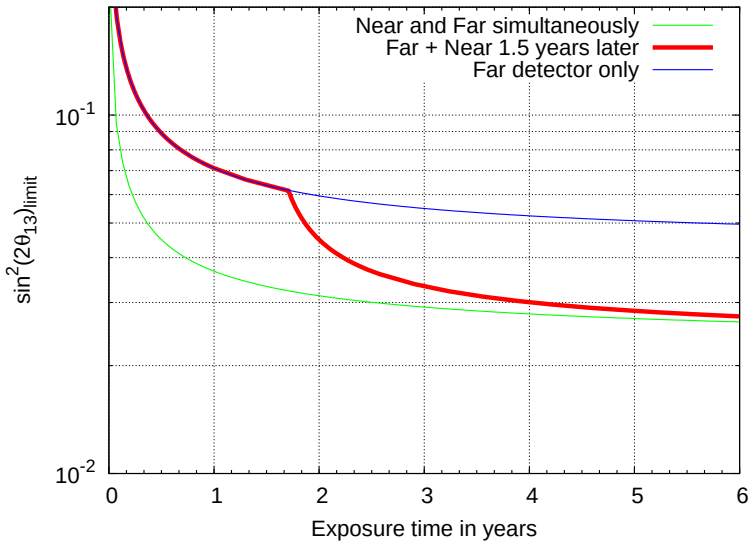

Figure 8: $\sin^2(2\theta_{13})$ sensitivity limit vs. time for the planned detector-installation scenario

PXE based scintillator was measured as a function of dodecane concentration. A scintillation yield of 78% with respect to pure PXE is observed at a volume fraction of 80% dodecane. Pure phenyldodecane or pseudocumene based mixtures could be used as scintillator solvent as alternatives to the PXE/dodecane mixture.

Metal loading of liquid scintillators has been comprehensively studied at MPIK and LNGS/INR for several years. Research with gadolinium loaded scintillators in both institutes indicates that suitable scintillators can be produced. Two scintillator formulations have been investigated, one based on carboxylic acids and the other on Gd-β-diketonates. Both systems show good performance and are viable candidate liquid scintillators for the $\overline{\nu}_e$ target.

During the first CHOOZ experiment, the Gd-loaded scintillator used in the ν target showed a rapid and unexpected degradation in transparency, which has been ascribed to oxidation by nitrate ions [15]. In Double Chooz the long-term stability of the target scintillator is of fundamental importance, both to assure a sufficiently long running time (several years) and to avoid systematics due to a possible different evolution of the liquids in the two detectors.

The Heidelberg and Gran Sasso groups of the Double Chooz collaboration have been producing Gd-loaded scintillator since 2003. A large number of samples have undergone extensive monitoring of their chemical stability, in the laboratories where these scintillators have been synthesized, and especially at Saclay. The best formulations, developed during 2005, have shown no degradation at all during $\approx$1 year survey time, while some worsening of the transmission has been observed at elevated temperature. It is not possible to correlate the results of the two tests by defining some "acceleration factor". In general, the Gd-carboxylate scintillators have shown a worse performance at high temperature. These systems, however, are expected to be more fragile with respect to strong temperature variations, since synthesis is based

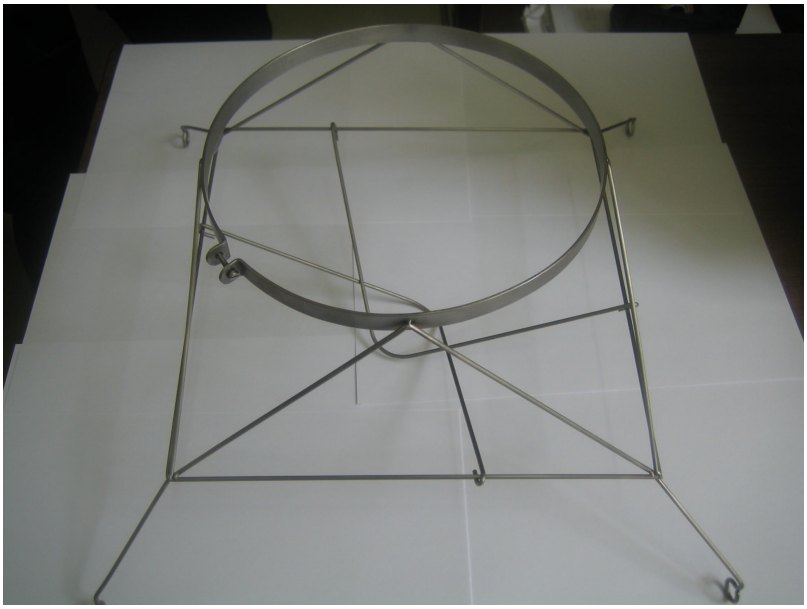

Figure 9: Mock up of the PMT supporting structure done at CIEMAT.

on chemical equilibrium. The parameters of the synthesis are tuned to drive this equilibrium toward stability at room temperature, which does not necessarily imply stability at elevated temperature. In the case of the beta-diketonate system, instead, the degradation is believed to be due to the accelerated reactivity of impurities left from the synthesis.

The γ-catcher liquid was chosen to match the density and at the same time the light yield between the inner two volumes. The scintillator contains 10% PXE, 30% mineral oil and 60% dodecane. As in the target a PPO/bis-MSB combination was chosen to shift the light into the near UV and visible regions.

1.8 Phototubes

A full discussion of the phototube system to be used in Double Chooz may be found in Section 4 of the Full Collaboration Double Chooz Proposal [1]. The target and γ-catcher volumes of each of two identical Double Chooz (DC) detectors will be viewed by a system of photomultiplier tubes (PMTs) installed in the non-scintillating buffer volume. This inner PMT system will provide the event energy and time measurement as well as the trigger. The design of the PMT system for Double Chooz has been developed by the US-DC group and was described in previous DC publications [3, 1]. Construction of the PMT system in the Double Chooz experiment will be a shared effort among France, Spain, the US, and Japan. The US group is planning to contribute to the DC PMT system in the following aspects: (a) evaluation and testing of the PMTs; (b) participation in installation and commissioning of PMT system; (c) measurements of PMT radiopurity; (d) design and measurement of PMT magnetic shielding.

Following the successful operation of CHOOZ with 15% photocathode coverage

by 8" PMTs, we plan a similar photocathode coverage (effectively ~13.5%). Average light collection is to be above 180 p.e./MeV.

The goal for the detector trigger threshold is ≈0.5–0.7 MeV (with 90% efficiency at 0.8 MeV and ≥ 99.97% at 1.0 MeV) that will allow high-efficiency detection of antineutrino events independent of the systematics of energy-scale non-linearity and calibration. In the CHOOZ detector [15] the trigger threshold for prompt signal detection was chosen at 1.3 MeV. This resulted in a raw trigger rate of ≈130 Hz that after applying software cuts was reduced to ≈65 Hz. Lowering the trigger thresholds in CHOOZ was limited by the DAQ bandwidth. In the Double Chooz detectors the singles rate situation will be considerably improved by introducing passive 17-cm iron shielding around the detector (see section 1.7.2). Also, a passive 1062-mm-thick buffer layer of non-scintillating oil (+12-15 mm of acrylics) is being introduced between the scintillator and the wall on which the photomultiplier tubes are mounted. Radioactivity of the liquid scintillator and buffer oil will be controlled by the purification process during the liquid scintillator production and at detector filling time. The effect of radioimpurities is discussed in more detail in section 1.6.3. In addition to the above, the radioassay and careful selection of the construction materials will help to further reduce the singles rates.

1.8.1 PMT Performance

Light produced in the liquid scintillator of the Double Chooz far- and near-detector targets will be detected by two identical photomultiplier (PMT) systems. The number of phototubes (534 per detector) and their geometrical arrangements will be the same for both detectors. With individual PMT thresholds of 0.25 spe (single photoelectrons) one can expect the following global PMT system performance characteristics:

- light output and uniformity of detector response: minimum response of 180 spe/MeV in the center of the detector increasing by less than 10% (to 200 spe/MeV) at the periphery of the target volume (5% is the predicted value). (This dependence is correctable by reconstruction of the spatial position of the event in the scintillator volume;)
- expected accuracy of vertex reconstruction ≈ 9 cm$/\sqrt{E(\mathrm{MeV})}$ in x, y, z projections;
- expected energy resolution $\approx 7.5\%/\sqrt{E(\mathrm{MeV})}$;
- PMT dark rate is expected to contribute ~ 1 count per second at the global energy threshold of 50 keV. We plan for the trigger threshold to be set at ≈ 0.7 MeV as determined by radiopurity considerations.

1.8.2 Sensitivity to Magnetic Field

The performance of PMTs is sensitive to a magnetic field. As an example Figure 10 shows the typical effect from the Earth's magnetic field transverse to the PMT axis

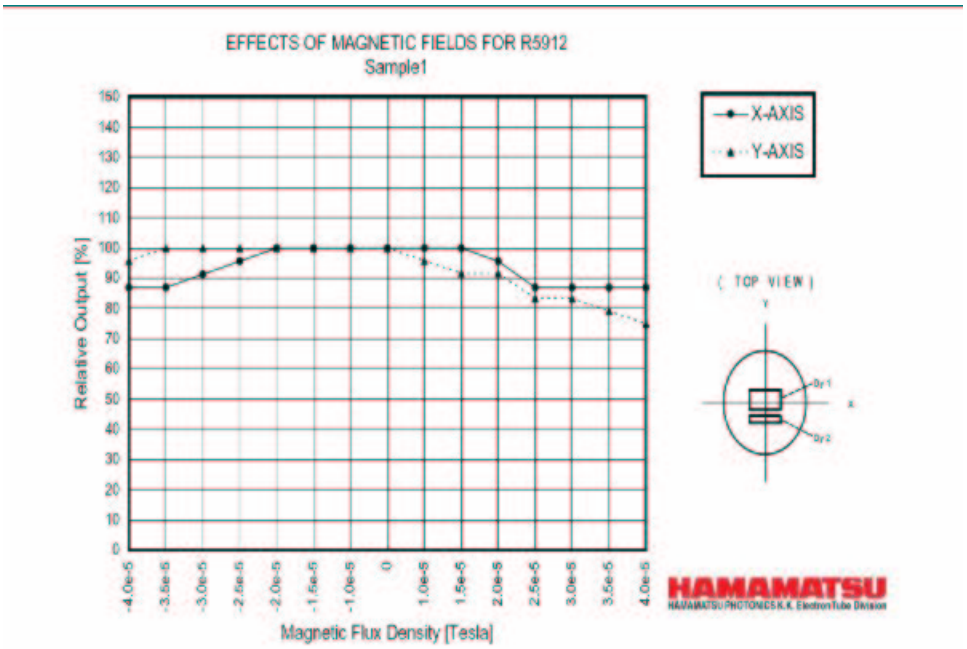

Figure 10: Effect of transverse magnetic field on 8-inch PMT response (measurements provided by Hamamatsu Corporation).

on one of the candidate PMTs (Hamamatsu R2512) [21]. It is expected that PMTs of other manufacturers will have similar sensitivity to the transverse magnetic field. Magnetic field as known from geomagnetic models [22] has the following components at the Chooz location: 0.43 G Down, 0.20 G North, 0.003 G West. Unshielded magnetic field transverse to the PMT axis can create a response difference up to 30% for the tubes at various locations in the detector. These differences in PMT response can potentially affect the identicality of the two Double Chooz detectors and thus should be eliminated or reduced. The presence of the 17-cm iron shield around the detector, needed for the reduction of external radioactivity counts by the scintillator, might result in additional non-uniform magnetic field inside the detector at the locations of the PMTs. The collaboration plans to demagnetize individually each iron bar prior to installation in the shielding assembly; however, the absence of non-uniform residual local fields up to 2 G after demagnetization is not guaranteed. In addition, iron bars can be slowly re-magnetized by the Earth's magnetic field. Thus, magnetic shielding of the individual photomultipliers with mu-metal will be required. The acceptable residual transverse magnetic field is < 0.05 G at any PMT location in the detector. Most sensitive to the magnetic field is the gap between the photocathode and the first dynode. If a mu-metal cylinder is used for PMT shielding it is known that the cylinder should extend beyond the PMT cathode for at least one cylinder radius. Such shielding for hemispherical phototubes will substantially restrict their viewing solid angle. In order to compensate for the reduction of the solid angle introduced by mu-metal shielding we plan to install Winston-cone light

concentrators attached to the PMT support structure.

2 Budget

2.1 Overview of Costs

As of July 1, 2006, the laboratory previously used by the CHOOZ experiment has been made available to the Double Chooz collaboration. The relationship between the CHOOZ experiment and Electricite de France (EdF) was very cooperative and cordial; the success of a θ_{13} experiment such as Double Chooz requires such close cooperation. EdF has indicated that it will again be a willing partner in cutting-edge neutrino science.

The current estimate for the full cost of both detectors (not including the near detector lab) is 9.0-9.5 million euros. In France, IN2P3 and CEA/Saclay have approved a contribution of 2.2-2.5 million euros. The collaboration also includes Germany, Japan, Spain, Russia and the United Kingdom. In October 2004, there was a U.S. request for $4.858M [3], primarily for phototubes, electronics and an outer veto system for the near detector. That request has not been acted upon and some of that scope has been assumed by others. In this document, we are requesting DOE construction funding of $1.377M primarily for electronics and calibration activities. (Please note that this figure is fully loaded and includes escalation.) These crucial parts of the experiment coincide with the expertise of the U.S. collaborators, who have extensive experience with these systems in previous reactor neutrino experiments.

2.2 Work Breakdown Structure (WBS)

The Chooz-U.S. scope, consisting of cost, schedule and an understanding of U.S. participation, is driven by the European project completion date of April 2008. The contributions are separated into three major elements: Electronics, Calibration and Monitoring Systems. We provide here a description of those elements, the cost structure for those elements, escalation considerations, and a schedule to meet Double Chooz goals. The following describes U.S. contributions to the Double Chooz project. These contributions provide essential components, functionality, and assured integration of U.S. and European systems.

1. **Electronics**

   1.1 HV Splitter

   The exact number depends on whether there will be any summing of detector channels, but it is expected that individual high voltage will be provided for every channel. Since the same cable is used to carry the signal from and high voltage to each phototube, splitter boxes are required to remove the signal at low voltage. The task to assemble and test HV splitters is to be performed at the University of Tennessee, in close cooperation with Drexel.

   1.2 Analog Front End Electronics

Based on requirements for 1024 phototubes, provides the electronics for readout of all phototubes in the near and far Double Chooz detectors plus 20% spares. It will include assembly and testing at Drexel and installation at the near and far detector laboratories for Double Chooz in France.

1.3 PMT Rate Monitor

The PMT monitoring is to provide periodic samples of PMT singles rates at a sub-photoelectron threshold, with readout and alarm software integrated into the main DAQ. Assembly and testing will be performed at the University of Tennessee, and installation at the Double Chooz laboratories.

2. **Calibration Systems**

2.1 z-axis Deployment System

Provides for a system to deploy radioactive sources along the z-axis of both the far and near detectors. The required glove boxes above the detector will be designed at Sandia and constructed at the University of California-Davis. The fish line deployment system will be designed and produced at Davis in cooperation with the University of Alabama.

2.2 Articulated Arm System

Provides for the accurate deployment of calibration sources throughout the target regions of the detectors. The articulated arm system will be developed at a later time than the z-axis deployment system, to allow initial calibrations along the z-axis and help drive the final requirements of the articulated arm system. The development and assembly will be done by the Argonne National Lab, with assistance from the University of Alabama.

2.3 Guide Tube System

Provides for deployment of calibration sources in the gamma catcher. A wire driver will be built for accurate deployment by the University of Alabama.

2.4 Laser System

Provides for a laser system to quantify and monitor pertinent properties of each photomultiplier. The system will be developed and tested at the University of Alabama and installed in the Double Chooz laboratories.

2.5 Radioactive Source Production

Provides for the procurement of source material and fabrication of deployable sources to be used with the fish line system, the articulated arm, and the wire driver guide tubes. A number of gamma and neutron sources are needed. These will be obtained by the University of Alabama.

3. **Monitoring Systems**

3.1 Environmental Monitoring

Based on requirements, provides a system to control and scan items such as thresholds, high voltage settings and temperatures, and to provide alarms, warnings and diagnostic information to the experiment operators. This provides for the purchase from Maxim IC/Dallas Semiconductor of 1-Wire interface chips and other components needed to control and read back hardware. Assembly will take place at Kansas State University and installation at the Double Chooz laboratories.

3.2 Radiopurity Monitoring

Based on requirements, components of systems that will be inside the steel tank will be tested at the Oroville Low Background Counting Facility. This facility is operated by the Lawrence Berkeley National Laboratory. Sandia National Laboratories will coordinate this survey, collect samples and analyze the results.

2.3 Cost & Schedule Details

The cost estimation for the Chooz-U.S. project was made on the basis of the requirements for each WBS system. The estimates were generated by specific engineers or supervising physicists with previous experience from other similar projects. Where possible, quotes from commercial vendors and catalog information were used for costs related to materials and sub-contracted services. The following assumptions were made:

1. U.S. systems will not be subject to any taxes or tariffs for shipping and installation at the experimental site in France.

2. The French laboratory at Chooz will provide all suitable skilled technician labor necessary for installation.

3. All M&S estimates are free of overhead costs, consistent with the regulations of the participating universities.

4. Estimated effort rates are fully burdened with respect to the listed institution.

5. No overtime rates are assumed for the duration of the project.

6. The effort cost listed for each task refers to the incurred costs which are over and above the base operating funding supplied by the DOE.

7. All costs are listed in FY05 dollars and escalated to then-year dollars, FY06-09.

8. All costs listed here are being requested from the DOE and do not include the proposal by Columbia and Chicago groups for NSF funding of an outer muon tracker. Together the DOE and NSF proposals represent a coherent U.S. program to understand backgrounds and systematic errors in the first reactor experiment dedicated to a search for θ_{13}.

Detailed cost estimates have been calculated and are available. Additional details such as specific component costs, written quotes, catalog pricing, and detailed drawings are also available. Escalation has been calculated for M&S based on the CBO Consumer Price Index, and for labor based on the Employment Price Index.

WBS	description	year 1	year 2	year 3	year 4	totals
1.1	HV splitter	$0	$26,923	$84,976	$87,823	$199,722
1.2	Analog Electronics	$183,487	$81,687	$37,429	$721	$303,325
1.3	PMT rate monitor	$0	$46,358	$45,769	$42,960	$135,087
2.1	z-axis deployment	0	$45,091	$51,152	$26,563	$122,805
2.2	Articulated Arm	$0	$0	$174,776	$36,054	$210,830
2.3	Guide Tubes	$1,306	$53,363	$0	$0	$54,670
2.4	Laser System	$0	$72,068	$0	$44,912	$116,979
2.5	Radioactive Sources	$0	$17,772	$29,484	$3,948	$51,203
3.1	Environmental Monitor	$0	$43,742	$2,311	$8,545	$54,598
3.2	Radiopurity Monitor	$0	$24,520	$0	$25,818	$50,339
	Management	$13,548	$51,071	$13,000	$250	
	Totals	$198,342	$462,595	$438,896	$277,594	$1,377,427

Table 12: Chooz-US Cost Profile. The costs are shown for each major task over the expected 4 years of the project (defined from July 1 2006 to June 30 2010.). The listed costs are in then-year dollars and contain the contingencies described in the detailed budget description. Also included are the cost of initiating subcontracts to institutions, which at U.C. Davis is 51.5% (52.0%) on the first $25,000 for subcontracts starting in year 1 (year 2,3,4).

2.4 Project Management

The Double Chooz Spokesperson is Herve de Kerret from APC and PCC College de France who has overall responsibility for Double Chooz. Technical and Project Management for the full collaboration takes place at Saclay. The Project Manager is Florence Ardellier. Collaboration policy is set by an executive committee consisting of two representatives from each country, France, Germany, Spain, U.K., and the U.S.

The Chooz-U.S. collaboration will operate as an integral part of Double Chooz, but for reporting and management purposes, a Chooz-U.S. structure will be maintained. The principal investigator from each institution in the U.S. will be a member of the Institutional Committee, which has the responsibility of electing the U.S. co-spokespersons. To coordinate laboratory and university efforts the Institutional Committee is initially electing two U.S. Co-Spokespersons. Maury Goodman is a physicist at Argonne National Laboratory and a recognized leader on the Soudan 2 experiment. He was also spokesman for P-822, the original proposal for a long-baseline neutrino beam at Fermilab. Prof. Robert Svoboda is a senior professor

at University of California-Davis and was Co-Convener for Solar Neutrinos on the Super-Kamiokande experiment and University Coordinator for the construction of the KamLAND detector. They will carry overall responsibility for all technical and budgetary aspects of Chooz-U.S. contributions. They will also be responsible for coordinating the overall project with the European collaborators and will report to the host country spokesperson on the overall progress of the U.S. construction effort. The institution responsible for financial management of the project will be the University of California, Davis (UCD). This will be accomplished via subcontracts from UCD to the institutions responsible for producing the detector components. Costs for initiating these subcontracts are included in the project budget.

Last Update: Tuesday, September 12, 2006

Project Funding

	Description	Institution	Baseline M&S Costs FY06	FY07	FY08	FY09	Total	Cont	Baseline Effort Costs FY06	FY07	FY08	FY09	Total	Cont	Fully Loaded Totals FY06	FY07	FY08	FY09	Total
0	Total Project		$136,600.88	$232,774.86	$197,811.44	$161,466.47	$728,653.65	17%	$14,628.75	$90,655.75	$123,310.50	$54,094.00	$282,689.00	27%	$184,794.22	$411,523.59	$425,897.93	$277,344.34	$1,299,560.09
1	**Electronics Systems**																		
1.1	HV Splitter		$0.00	$4,096.16	$46,156.61	$46,437.65	$96,690.42	17%	$0.00	$17,842.00	$20,704.50	$20,937.00	$59,483.50	18%	$0.00	$26,922.85	$84,975.77	$87,823.13	$199,721.76
1.2	Analog Electronics		$135,719.18	$48,441.47	$28,908.49	$568.72	$213,637.86	18%	$14,628.75	$16,203.75	$675.00	$0.00	$31,507.50	26%	$183,487.82	$81,686.60	$37,429.14	$721.31	$303,324.87
1.3	PMT Rate Monitor		$0.00	$27,621.78	$28,100.14	$27,533.14	$83,255.06	11%	$0.00	$10,770.00	$7,833.00	$5,673.00	$24,276.00	21%	$0.00	$46,358.00	$45,769.32	$42,959.90	$135,087.22
2	**Calibration Systems**																		
2.1	Z-axis Deployment System		$0.00	$28,102.00	$38,471.00	$21,438.00	$88,011.00	15%	$0.00	$6,880.00	$2,384.00	$1,184.00	$10,448.00	37%	$0.00	$45,090.56	$51,152.48	$26,562.78	$122,805.83
2.2	Articulated Arm System		$0.00	$0.00	$32,300.00	$7,830.00	$40,130.00	32%	$0.00	$0.00	$90,394.00	$17,380.00	$107,774.00	29%	$0.00	$0.00	$174,776.18	$36,053.98	$210,830.16
2.3	Guide Tube System		$881.70	$14,839.79	$0.00	$0.00	$15,721.49	20%	$0.00	$22,000.00	$0.00	$0.00	$22,000.00	48%	$1,306.40	$53,363.29	$0.00	$0.00	$54,669.69
2.4	Laser System		$0.00	$61,145.50	$0.00	$35,998.00	$97,143.50	14%	$0.00	$0.00	$0.00	$0.00	$0.00	0%	$0.00	$72,067.60	$0.00	$44,911.64	$116,979.24
2.5	Radioactive Source Production		$0.00	$14,600.00	$23,700.00	$5,600.00	$43,900.00	17%	$0.00	$0.00	$0.00	$0.00	$0.00	0%	$0.00	$17,772.10	$29,483.91	$3,947.91	$51,203.91
3	**Monitoring Systems**																		
3.1	Environmental Monitoring		$0.00	$22,451.60	$175.20	$4,584.40	$27,211.20	27%	$0.00	$9,360.00	$1,320.00	$1,320.00	$12,000.00	42%	$0.00	$43,742.11	$2,311.13	$8,545.28	$54,598.52
3.2	Radiopurity Monitoring		$0.00	$11,476.56	$0.00	$11,476.56	$22,953.12	22%	$0.00	$7,600.00	$0.00	$7,600.00	$15,200.00	13%	$0.00	$24,520.48	$0.00	$25,818.41	$50,338.89

CBO Year-by-Year Inflation Projections	2006	2007	2008	2009
Consumer Price Index	1.9%	2.1%	2.2%	2.2%
Employment Price Index	3.3%	3.3%	3.3%	3.3%

Additional Contributions from Base Funding

	Description	Institution	Baseline M&S Costs FY06	FY07	FY08	FY09	Total	Cont	Baseline Effort Costs FY06	FY07	FY08	FY09	Total	Cont	Fully Loaded Totals FY06	FY07	FY08	FY09	Total
0	Total Project		$0.00	$42,721.20	$43,443.60	$58,653.60	$144,818.40	28%	$25,830.00	$66,907.50	$12,648.00	$16,973.50	$122,359.00	31%	$35,227.77	$131,829.84	$76,090.10	$101,162.96	$344,310.67
1	**Electronics Systems**																		
1.1	HV Splitter		$0.00	$0.00	$13,986.00	$13,986.00	$27,972.00	29%	$0.00	$14,098.00	$4,713.50	$4,636.50	$23,448.00	17%	$0.00	$17,266.95	$25,339.05	$25,868.81	$68,474.82
1.2	Analog Electronics		$0.00	$22,260.00	$12,900.00	$9,360.00	$44,520.00	27%	$13,200.00	$9,127.50	$4,117.50	$0.00	$26,445.00	28%	$17,665.07	$41,952.16	$23,140.87	$12,890.20	$95,648.30
1.3	PMT Rate Monitor		$0.00	$0.00	$9,374.40	$9,374.40	$18,748.80	25%	$0.00	$5,522.00	$3,817.00	$2,937.00	$12,276.00	20%	$0.00	$6,773.28	$17,727.60	$16,892.41	$41,393.30
2	**Calibration Systems**																		
2.1	Z-axis Deployment System		$0.00	$0.00	$0.00	$0.00	$0.00	0%	$11,880.00	$740.00	$0.00	$0.00	$12,620.00	37%	$16,812.69	$1,081.81	$0.00	$0.00	$17,894.51
2.2	Articulated Arm System		$0.00	$0.00	$0.00	$3,720.00	$3,720.00	24%	$0.00	$0.00	$0.00	$0.00	$0.00	0%	$0.00	$0.00	$0.00	$5,008.73	$5,008.73
2.3	Guide Tube System		$0.00	$3,720.00	$0.00	$3,720.00	$7,440.00	28%	$750.00	$21,300.00	$0.00	$0.00	$22,050.00	48%	$750.00	$26,250.22	$0.00	$5,170.42	$32,170.64
2.4	Laser System		$0.00	$11,310.00	$0.00	$11,310.00	$22,620.00	29%	$0.00	$15,800.00	$0.00	$9,400.00	$25,200.00	36%	$0.00	$30,958.09	$0.00	$25,232.39	$56,190.48
2.5	Radioactive Source Production		$0.00	$0.00	$0.00	$0.00	$0.00	0%	$0.00	$0.00	$0.00	$0.00	$0.00	0%	$0.00	$0.00	$0.00	$0.00	$0.00
3	**Monitoring Systems**																		
3.1	Environmental Monitoring		$0.00	$5,431.20	$7,183.20	$7,183.20	$19,797.60	29%	$0.00	$320.00	$0.00	$0.00	$320.00	42%	$0.00	$7,547.32	$9,882.58	$10,100.00	$27,529.89
3.2	Radiopurity Monitoring		$0.00	$0.00	$0.00	$0.00	$0.00	0%	$0.00	$0.00	$0.00	$0.00	$0.00	0%	$0.00	$0.00	$0.00	$0.00	$0.00

3 Calibration

Precise calibration is essential to sensitive neutrino disappearance experiments. We propose to provide the calibration system for the Double Chooz experiment as one of our main responsibilities. This responsibility would be appropriate given our extensive experience in calibrating the Palo Verde, CHOOZ, Super-Kamiokande, KamLAND, and MiniBooNE detectors. In what follows, we first describe the calibration goals for the experiment and then outline the basic components of the system that we propose to provide.

3.1 Calibration Goals

The two main tasks for which calibration is critical are the estimate of the inverse beta decay detection efficiency and the determination of the energy scales for positrons, gammas, and neutrons. We quantify each of these goals in turn below.

The relative detection efficiency between the near and far detectors should be known with an uncertainty less than 0.5% including all deadtime effects. The uncertainty budget for the relative detection efficiency is taken to be (a) 0.2% from the energy cut ("6 MeV cut") applied to select neutron candidates, (b) 0.1% from the cut on the neutron capture time, (c) 0.25% from deadtime, and (d) <0.2% from the requirement (if used) of spatial correlation between the prompt and delayed subevents.

With regard to energy scales, the tolerable uncertainty depends on the level and nature of backgrounds. We have adopted 1% as the maximum uncertainty on the absolute energy scales for gammas and positrons because it is realistically achievable; the corresponding relative uncertainties between the near and far detectors should then be much less than 1% since the same energy-scale determination methods will be used for both detectors. For the neutron energy scale, a less stringent requirement suffices: the uncertainty in the estimate of the visible neutron kinetic energy should be limited to 20%. This relaxed requirement reflects the large signal-to-background ratio expected for each detector as well as the mild energy dependence of the fast-neutron background across the reactor-neutrino energy range.

It is practically unavoidable that calibrations probe the detectors under different conditions than do the signals and backgrounds of interest. It is likely not feasible to build and deploy inverse beta decay sources, and even the detector responses to positrons and neutrons separately cannot be directly measured. For example, the typical energies of neutrons produced in inverse beta decay induced by reactor neutrinos are tens of keV, whereas the energies of neutrons produced by available calibration sources lie above 1 MeV. Moreover, the calibration process introduces structures into the detector that are not present during normal data taking. It is therefore necessary to use detector simulation to estimate the detector response to inverse beta decay and relevant backgrounds; the role of calibration is then to provide the information needed for tuning and checking the simulation to the required accuracy. Included in this process is correcting the calibration data for the effect of structures introduced into the detectors for calibration.

In addition to providing measurements of detector response that will control its uncertainties within the levels stated above, the calibration program must provide information that can be used to check assumptions about other aspects of detector performance and to carry out analyses using different sets of selection criteria or alternate methods of background subtraction. Specifically, the scope of calibration will also include the following:

1. A check that the trigger is fully efficient for inverse beta decay events.

2. Calibration of the efficiency of a spatial correlation cut to within 0.2%.

3. Measurement of the detector response to neutrons, for modeling the background due to fast neutrons.

As is clear from the foregoing description, the calibration goals apply in large part to the relative performance of the near and far detectors. Some errors in absolute calibration of each detector may thus be tolerated so long as they cancel between the two detectors. The calibration program described below, however, is conservative in the sense it is designed to approach the stated calibration goals in the absolute sense for each detector and not only strive to reach the goals in the relative sense between the two detectors. The reason is twofold: (1) such a program can be pursued with a reasonable level of resources and effort, and (2) given the importance of calibration to high sensitivity to θ_{13} in a reactor experiment, reliance on cancellation of errors should be kept to a minimum. To help ensure that any residual errors in absolute calibration cancel between the two detectors, the same calibration sources will be deployed in both detectors and the deployment methods will be identical.

The following sections describe the basic components we would provide and the role they would play in meeting the calibration goals. These components include a a set of certified sealed sources (section 3.2); a laser flasher system (section 3.3); a z-axis source deployment system(section 3.4.2); an articulated arm (AA) system to deploy sources off the z-axis (section 3.4.3); a set of source tubes and wire driver system to deploy sources in the gamma catcher (section 3.4.5); and gloveboxes and clean areas for source deployment (section 3.5).

3.2 Radioactive Sources

3.2.1 Gamma Sources

Gamma sources will be used for the following purposes:

1. Precisely measure the response of scintillator (target and γ-catcher) to gammas from well below inverse beta decay threshold to at least $\approx$5 MeV. Spanning this range and beyond will also facilitate understanding the roles of quenching and Cerenkov radiation, uncertainties in which propagate through to the uncertainties in the positron energy scale derived from the gamma energy scale.

2. Measure light transport properties (absorption, reemission, speed of light) of the liquids in the target, γ-catcher, and buffer.

Table 13: Gamma sources to be used in calibrating Double Chooz

	Source	E_γ (MeV)	Half-life
1	^{203}Hg	0.289	46.6 d
2	^{137}Cs	0.667	30.1 y
3	^{68}Ge	0.511 + 0.511	271 d
4	^{60}Co	1.333 + 1.173	5.27 y
5	n capture on H	2.223	
6	n capture on C	4.94	

3. Measure relative PMT timing offsets.

4. Check relative efficiency of far and near detectors with respect to trigger, data acquisition, event reconstruction, and event selection.

5. Monitor detector stability.

The set of gamma sources to be used is enumerated in Table 13. There will be significant continuum background due to n capture on Gd underlying the 4.94 MeV line and hence it is likely to be visible only for long source deployments. The feasibility of deploying other high-energy gamma sources is being explored.

Detector simulations have been carried out to estimate how the detector response to gammas will vary with position. The results are typified by what is shown in Figure 12 for samples of 1 MeV gammas generated along the x-axis. The strongest variations occur near the target–γ-catcher boundary and across the γ-catcher. To avoid unacceptable uncertainties in energy reconstruction, the deployment system will have the capability to position gamma sources near the target–γ-catcher boundary and at points within the γ-catcher. Furthermore, toward ensuring that the uncertainty in the energy reconstruction due to position uncertainty is well below 1%, the systematic uncertainty in source position must be less than 1.5 cm. The particular choice of deployment positions in the γ-catcher will be further discussed in connection with calibrations with neutron sources.

3.2.2 Neutron Sources

Neutron sources will be used for the following purposes:

1. Measure the relative neutron detection efficiency between the two detectors.

2. Measure the absolute neutron detection efficiency at selected points in each detector. Such a measurement is required to help check the accuracy of the neutron simulation and for analysis of data for which there is only one detector, most notably the far detector data taken before the near detector is turned on.

3. Measure the energy response of the target and γ-catcher to neutrons, to enable accurate simulation of the prompt energy spectrum of fast neutron events.

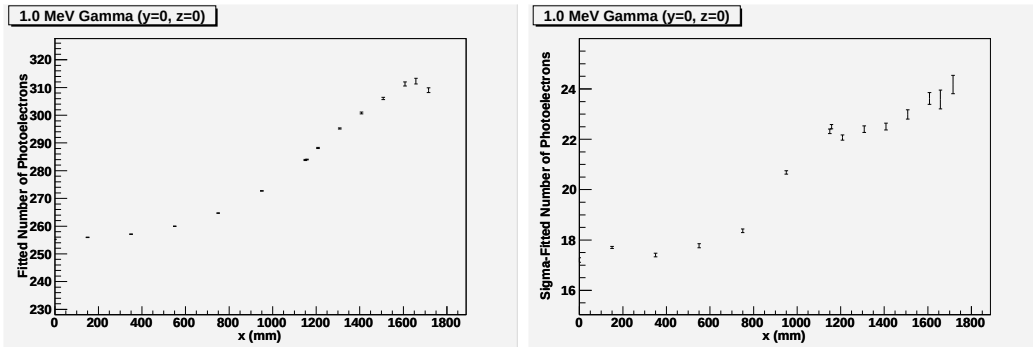

Figure 12: Center (left) and sigma (right) of Gaussian fits to peak in photoelectron distribution versus distance along the x-axis for 1 MeV gammas.

4. Improve understanding of deadtime effects for inverse beta decay detection efficiency by studying deadtime effects on event correlations in neutron calibration events. Neutron calibration events are comprised of (i) a prompt deposit of neutron kinetic energy and energy of gammas accompanying neutron emission and (ii) delayed deposits of energy from gammas released by one or more neutron captures.

To measure the absolute efficiency, deployment of a source instrumented with a dedicated device to tag neutron emission, such as the one used in the CHOOZ experiment, is planned. Using the detector itself to tag neutron emission, by registering the prompt energy deposited by accompanying gammas, is under study. In order to measure the energy response of the detector to neutrons, the energy distribution of the neutrons emitted by each source must be well known and corrections must be made for the energy deposited by any gammas accompanying the neutron emission.

Detector simulation has been carried out at the photoelectron multiplicity and timing level to understand where neutron sources should be deployed and the degree of corrections that would have to be applied to the efficiencies measured with Cf-252 or Am-Be sources to obtain the efficiency for neutrons produced by inverse beta decay. Monoenergetic neutrons were generated uniformly throughout the target, uniformly throughout the γ-catcher, or at specific points. Several energies were simulated: 0.01 MeV as a characteristic energy for reactor neutrino events, 2 MeV as the approximate energy for Cf-252 neutrons, and 4 MeV, which is close to the mean energy for Am-Be neutrons. For each event, photoelectrons were classified as prompt or delayed, depending on whether they were registered less or more than 200 ns from the start of the event. The mean time of the delayed photoelectrons was used as the capture time. Neutron selection cuts were defined based on the total number of photoelectrons detected and the neutron capture time.

The following points can be drawn from the simulations performed to date:

- The neutron detection efficiency varies significantly throughout the target, hence the calibration system should have the capability to deploy neutron

sources throughout the target volume. Figure 13 shows the neutron detection efficiency as a function of distance to the target–γ-catcher boundary for neutrons generated uniformly in the target.

- Efficiency loss due to neutrons produced in the target escaping into the γ-catcher is termed "spill-out" while efficiency gain due to neutrons produced in the γ-catcher being captured on Gd in the target is termed "spill-in". For neutron sources such as Am-Be and Cf-252, spill-in and spill-out are separately large effects ($\approx$5%) but appear largely to cancel, as would be expected. However, since (a) the neutron detection efficiency is to be estimated with an uncertainty of a fraction of a percent and (b) the range of distance over which spill-in and spill-out occur is much greater ($\approx$20 cm) for Am-Be and Cf-252 sources than it is ($\approx$5 cm) for neutrons from inverse beta decay, deployment of neutron sources is planned both within the gamma catcher and in the target near the target–γ-catcher boundary, so as to measure this effect at representative points and help tune/check the MC simulation of neutron transport and capture.

- The neutron detection efficiency depends on the energy distribution of the neutrons. The differences in neutron detection efficiency between neutron sources and inverse beta decay are large enough that corrections must be applied in order to satisfy the requirements on uncertainty in detection efficiency. Multiple sources (Cf-252 and Am-Be), with different neutron energy spectra, will be deployed so as to measure and reduce this uncertainty. The possibility is also being explored of deploying a low-energy neutron source, in order to reduce the uncertainty in transferring efficiency measurements made at higher neutron energies to the energy range of neutrons produced by reactor neutrinos.

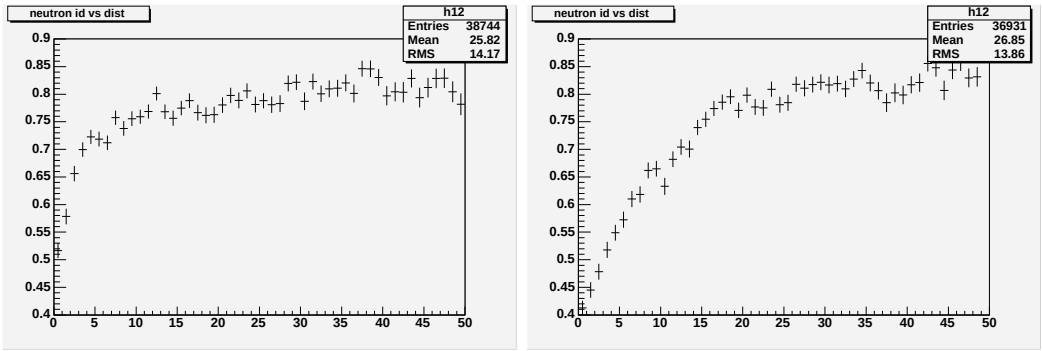

Figure 13: Neutron detection efficiency versus distance (in cm) between neutron creation point and target–γ-catcher boundary for neutrons generated in the target: (left) 0.01 MeV neutrons; (right) 4 MeV.

Detector simulation was also used to estimate the relative uncertainty in energy scale between the near and far detectors that could be tolerated while maintaining

an uncertainty of 0.2% in neutron detection efficiency due to the "6 MeV" cut. The energy-scale uncertainty so obtained is 100 keV.

3.2.3 Fabrication of Radioactive Sources

With the exception of a tagged Cf-252 source being built by the ITEP group, the scope for fabrication of the radioactive sources is included in the scope of this proposal. This proposed scope takes advantage of our experience in fabricating radioactive sources for the calibration of the Palo Verde and KamLAND experiments.

As listed above, the sources to be fabricated are Hg-203, Cs-137, Ge-68, and Co-60 for calibration with gammas and Am-Be and Cf-252 for calibration with neutrons. The requirements on fabrication of the sources include the following:

1. Each source can be deployed in the target and the buffer and in both the near and far detectors (universal deployability). Deployment of the same sources in all regions of the experiment to be calibrated significantly reduces the effect of uncertainties in source characteristics.

2. Source activities should be on the level of 100 Bq, in order to allow calibrations to be performed in a timely way without excessive DAQ deadtime or pile-up effects.

3. The sources must be compatible with all detector environments in which they are deployed and free of surface radio-contaminants and activity leaks.

The requirements of universal deployability, compatibility, and high radio-integrity constrain the capsule materials and geometries. For example, deployment of sources in the gamma catcher via guide tubes will limit the capsule diameter to a few mm and compatibility of the capsules with the Gd-loaded scintillator of the target is expected to severely limit what materials can be used for outer encapsulation.

Following tests of compatibility and deployment mechanics as needed, we will finalize the design of the source capsules and build the components at Alabama. In the case of gamma and Cf-252 sources, our expectation is that the capsule components will be sent to source vendors, who will insert the desired activities and then seal the capsules. In the case of compound sources such as Am-Be, we expect to fabricate them at the University of Alabama since sources of such small size are not readily available from source vendors and we have capability and experience in building such sources from stock.

Once the sources are fully assembled, characterization data will be taken to check that the output of the sources is as expected. HPGe, NaI, and neutron detectors, together with precise positioning jigs and calibrated reference sources, will be used to carry out this task. Following characterization, the sources will be thoroughly cleaned and then subjected to a radio-certification procedure. In this procedure, each source is soaked in weak nitric acid for several days and then the soak acid is counted with a low background Ge detector to check for radio-contamination with a sensitivity of a few mBq. (Weak nitric acid is preferred over liquid scintillator for

a soak liquid as we have shown that a broad range of radio-isotopes have a higher solubility in that acid than in scintillator.) A counting spectrum consistent with background is required for certification.

Radio-certification is the final step to be completed before the sources are shipped to the experiment site. At the experiment site, a special clean area will be set up for storing sources between deployments and preparing them for deployment. Provisions will also be made to keep the sources in a clean environment while being transported between the clean area and the detector into which they are to be deployed.

3.3 Laser Flashers

3.3.1 General Description

Fast lasers of several wavelengths will also be used to calibrate the detector. The main purpose is for vertex reconstruction, which depends critically on light transport and PMT timing. In principle, vertex reconstruction could be calibrated with gamma sources alone, but laser calibrations have the advantages of (a) providing signals of precisely known timing and amplitudes and (b) probing the response of the detector to specific wavelengths. Moreover, the laser systems can be designed to provide a wide range of well-known intensities, so that laser calibrations can be used to help interpolate the detector response between gamma calibrations and extrapolate it beyond the range of signal strength covered by gamma calibrations. The capability of lasers to provide very strong signals is useful in understanding the response of the detector to cosmic events, many of which excite the detector in a regime where the PMT response is expected to be significantly nonlinear. We have adopted the following as requirements for the laser calibration system:

- The laser light output must either be highly isotropic (preferred) or its anisotropy must be precisely known: this greatly simplifies the use of laser calibration data for light transport and energy calibration studies.

- The width of the laser pulse must be small compared to the scintillator decay times so that the distribution of photon arrival times at the PMTs does not depend strongly on the details of the laser pulse timing.

- At least two widely separated wavelengths must be provided: one that excites the scintillator to produce pulses with the same spectral and timing characteristics as those due to charged particles, and the other whose absorption length in scintillator is very long so that calibrations of PMT timing can be carried out with minimal complications due to re-emission and scattering.

- The dynamic range of the laser system must extend from much less than one photoelectron per PMT on average to several hundred photoelectrons per PMT.

- Fiber assemblies and diffusers must be selected so as to ensure that light is injected at precisely known points and the self-shadowing of the system is either negligible or adequately known.

Because of (a) the overlapping capabilities of calibrations with light flashers and those with radioactive sources and (b) the expectation that measurements of intrinsic PMT gain and timing characteristics will not depend significantly on the position of the source, deployment of the light flasher sources only on a vertical line through the target is sufficient. For the sake of simplicity, the symmetry axis of the detector is preferred, but deployment along another vertical line would also be suitable.

3.3.2 System Description

We propose to use two lasers at Double Chooz. The first laser will be a nitrogen laser operating at 337 nm, similar to the Spectra–Physics VSL-337 laser deployed at KamLAND and the original CHOOZ experiment. At this wavelength, photons will excite the scintillator and will produce re-emission with the same spectral and timing characteristics as a charged particle. This has the advantage that re-emission will be isotropic, limited only by self shadowing by the laser fiber tip. The intensity of the VSL-337 laser is very high, and will be controlled by two computer operated attenuators in series to achieve a large dynamic range. The attenuators will be calibrated in order to provide accurate knowledge of the relative amount of light per pulse in the detector. Nitrogen lasers of this type, produced by Spectra-Physics, feature pulse times of 1 ns, or less (FWHM). They also provide a logic pulse, generated from the light output, and with a timing accuracy of 1 ns which can be used to provide a laser event trigger. We will use a similar coupling between laser and fiber as the one used at KamLAND, which produces more than enough photons, simply by placing the end of the fiber behind a diffuser screen. Both the laser and the input end of the fiber will be mounted on an optics table and placed inside a light-tight protective box.

The second laser will be used primarily for PMT timing studies. This will require a laser with a longer wavelength so that it does not excite the scintillator. The laser pulse should also have better than 1 ns timing accuracy. Photons will be injected into the detector from a diffuser ball so that emission is isotropic. We have budgeted for a Picoquant diode laser at 470 nm, which can achieve both of these requirements and produce light at a wavelength closely matched to the PMT efficiency peak. Light from the laser will be transmitted to a fiber through a connector unit and delivered directly to the detector. Attenuation will be provided by manually placing neutral density filters inside the connector unit.

Light from both laser systems will be sent to the detector glovebox along a quartz fiber. Inside the glovebox the fiber will be connected to a laser reel containing a repository of aluminum coated fiber inside a Teflon tube. We will build two portable laser reels (one for each laser), which can be placed in the glovebox for deployment, and then removed. (A set of two laser reels will be built for each detector.) The laser reel for the UV laser will have a bare fiber at the end, while the other will incorporate a diffuser ball. Figure 14 shows a block diagram of the system.

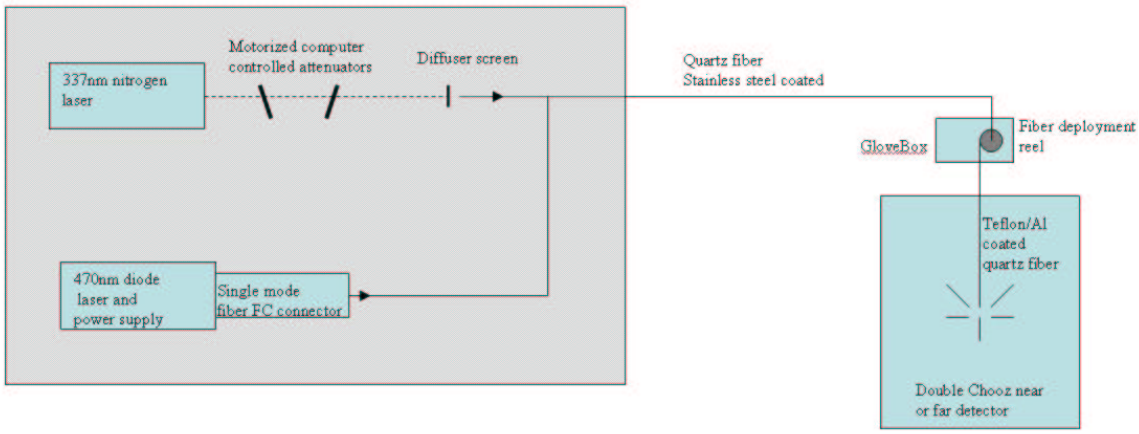

Figure 14: Schematic of the laser system.

3.4 Calibration Deployment

The purpose of the calibration deployment system is to deploy calibration sources into the target and γ-catcher regions. The calibration sources, the motivation for using them, and basic deployment requirements have been described above. The deployment systems utilized by the near and far detectors will be identical.

The deployment system must be designed to accommodate gamma sources, terminated fibers illuminated by external lasers, and neutron sources (untagged and tagged). The characteristic dimensions of these sources will range from a few mm to a few cm, and their masses from a few tens to a few hundreds of grams. The calibration system must be capable of positioning sources at representative points in the target and γ-catcher with an uncertainty less than 1.5 cm.

The materials and geometry of the deployment system must be chosen to minimize uncertainties in the corrections for shadowing and absorption. Detector simulation studies have been carried out to set the maximum dimensions that can be used and still meet the energy-calibration uncertainty requirements. Each material used in the calibration system must be compatible with all elements of the detector environment to which it is exposed. Furthermore, measures must be taken to protect the detector from radio-contamination by the calibration systems. The process of deploying the calibration system must not affect detector performance. The setup of the calibration deployment system should not be awkward or time-consuming, hence calibrations that are carried out frequently will be largely automated.

We next describe the deployment system in three parts: deployment methods, detector interface, and control systems.

3.4.1 Deployment Methods Overview

The methods of source deployment for the target region will differ from that for the γ-catcher region because of the different geometries and different calibration requirements. For the target, deployment of radioactive sources will mostly be done by a simple winch and motor system only along the (vertical) z-axis. Due to the necessity of measuring spill-in/spill-out and energy resolution near the target/γ-catcher boundary, a second option will be deployment via an articulated arm (AA) system. This system will be designed to reach all parts of the target volume.

The laser fiber will be deployed in a method identical to that used at KamLAND (which was designed at LSU). This uses a custom-built manual windlass and an aluminum-jacketed quartz fiber housed in a Teflon sleeve.

Target calibration will require sources that are certified radiologically clean and a deployment environment that will be clean and under a dry nitrogen atmosphere. Thus it is necessary to have a glovebox interface with associated clean room on the detector top (section 3.5.1). Those components of the deployment system that come into direct contact with the scintillator will be checked for material compatibility. Components that will not come into direct contact with the scintillator but that will be exposed to its vapors must also be tested.

For the γ-catcher, deployment will be done via source tubes with a wire driver. This system will be set up and operated in the same clean room as the glovebox.

3.4.2 z-Axis System

It is planned to have a simple motor and windlass scheme similar to that in KamLAND, where it has worked well. This consists of a stepper motor mounted inside a glovebox (section 3.5.1). The motor will be mounted in a custom-built housing to avoid contact with the scintillator. The shaft will extend out of the housing through a Teflon sleeve to turn a "fishing" reel. A shaft encoder also in the housing will provide positive motor position indication. Teflon-coated stainless-steel wire will be wound on the reel, pass through a pulley, and terminate with a weight and source attachment on the "business end".

System control will be via a commercial software package run on a controller (or laptop) external to the glovebox. Cable positioning will be via a combination of the encoder and the use of visible fiducial marks on the cable itself.

The preliminary design for this system is being done by Sandia National Lab under the auspices of their work on Non-Proliferation detectors. Final design will involve specific adaptation to Double Chooz. Construction will be done at U.C. Davis, which is located in close proximity to Sandia.

3.4.3 Articulated Arm

Because we intend to use the entire volume of the target, the calibration sources must be deployable throughout the target region. This will be accomplished using an articulated arm shown schematically in Figure 15. The articulated arm is comprised of a telescoping vertical shaft, supported from the calibration interface above the

detector, with a fixed-length arm pivoting at the lower end. By adjusting the length and azimuthal angle of the telescoping shaft and the angular position of the arm, a source attached to the end of the arm can be deployed at any position within a cylindrical volume. During calibration, an operator will attach a calibration source to the source holder, deploy the source into the target at the desired positions, and then retract the source to the detector interface.

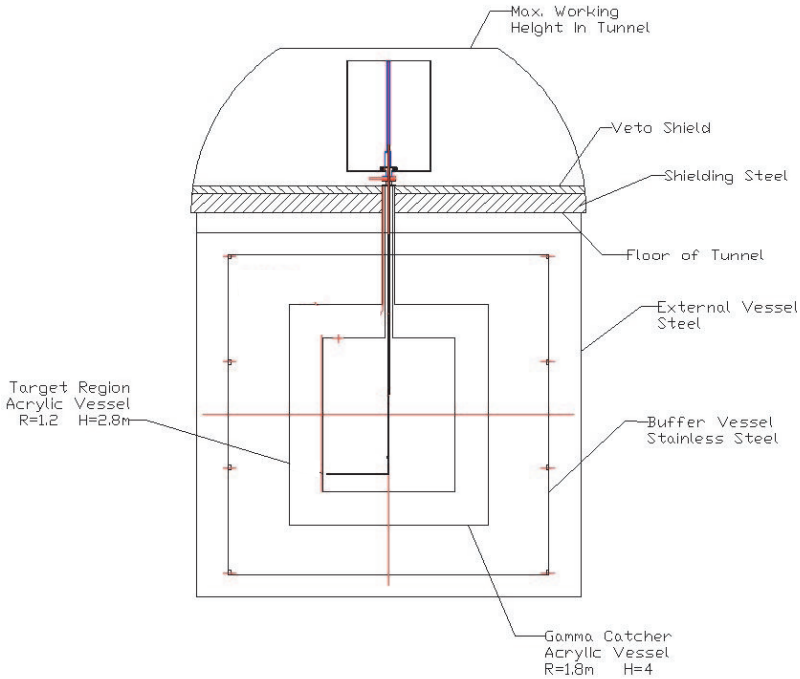

Figure 15: Schematic of the articulated arm system for deploying calibration sources throughout the target region.

The preliminary system design has been done at Argonne National Lab. The institutional responsibility for the final design work and construction has not yet been decided.

3.4.4 Laser Fiber Windlass

This is a fairly simple system and essentially identical to that used in KamLAND. It will be built by the University of Alabama along with the laser system itself.

3.4.5 Source Tube and Wire Drivers

The γ-catcher requires its own calibration because its light yield and properties of light and neutron transport will likely differ from those of the target. These differences can be measured using gamma and untagged neutron sources.

A guide tube system will be used to deploy calibration sources in the γ-catcher. The tubes must be small in diameter in order to avoid shadowing of scintillator light and to minimize dead material and absorption. The tubes will run into the γ-catcher from a manifold in the clean room enclosing the detector interface. Figure 16 shows a path that a guide tube could take in order to allow sources to be positioned at representative points within the γ-catcher. The calibration sources will be attached to a wire and pushed through the tube. In turn, the wire will be wound on a reel which is motor-driven under computer control.[2] The position of the source can be determined from the length of wire inserted into the tube and an accurate survey of the guide-tube geometry.

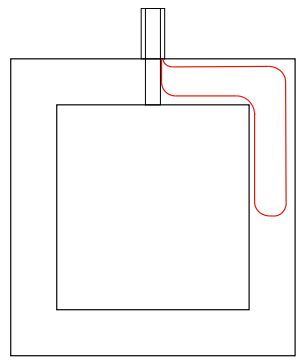

Figure 16: A possible guide-tube path for deployment of sources in the γ-catcher

The number of guide tube(s) to be deployed in the γ-catcher is being studied. The connection of the wire to the sources must be such that the same sources can be deployed in the γ-catcher as in the target. As with the deployment system for the target, all components will have to be checked for material compatibility before final selection and carefully cleaned before installation into the experiment. The wire source system will be set up and operated in the same clean room as the glovebox. The guide tubes, most likely made out of stainless steel, will be checked for leaks as the final step in their installation to ensure that the interior of the tubes is isolated from the scintillator. The two ends of each guide tube will be terminated in the clean room and a continuous flow of dry nitrogen through each tube will be maintained. The same cleanliness requirements will apply to sources and attached wires inserted into the tubes as apply for calibration sources deployed into the target.

This system will be built at the University of Alabama.

3.5 Detector Interface

The detector interface is the region that has access to the target and γ-catcher and that can be accessed from the outside to introduce and remove calibration sources.

[2] Wire source driver systems have been built for calibration of the CDF and ATLAS experiments. Prof. Virgil Barnes (Purdue) and collaborators have kindly provided us with essentially complete designs, which will be used as the starting point for the design of the Double Chooz system.

To prevent contamination of the detector, the detector interface will incorporate a glovebox for source manipulation and an airlock through which sources can be inserted and removed. The volume of the glovebox must be large enough that sources can be easily manipulated and the deployment system can be assembled and disassembled safely and easily as needed. The glovebox must be connected to an N_2 gas system and purged so that it has the same atmosphere each time it is opened to the detector. The glovebox will be equipped with radon and oxygen monitors for flagging leaks and monitoring the progress of purging. While the detector interface is open to the detector, it must also be light tight, which may mean that the operator must view the interior of the glovebox using infrared illumination and cameras. Feedthroughs for laser fibers and control and power cables must be hermetic. To bring sources into the detector interface, a transfer box is needed: sources are placed into this box through an external door, then the transfer box is purged, after which the operator opens an internal door and brings the source inside the detector interface.

3.5.1 Glovebox fabrication

Gloveboxes are commercially available that serve the needs of Double Chooz, however they will have to be modified for our particular requirements. A bottom access must be designed and constructed that will cap the top of the chimney. In addition, a "top hat" has to be made that will be tall enough to house the articulated arm. Internal hardware such as mounting brackets and bulkhead connectors must also be installed.

Sandia National Lab is undertaking the design of this glovebox system with technical assistance from Lawrence Livermore National Lab and in close collaboration with Saclay, who are designing the chimney, and with U.C. Davis, who will construct and test the system. Davis, Livermore and Sandia are in close proximity and are all working together on such projects.

Of concern in this system is material compatibility with scintillator. All materials used in the glovebox seals and viewports will be tested for such compatibility at Saclay.

3.5.2 Clean rooms

Covering the glovebox will be an $8' \times 8'$ soft-sided clean room. This is essentially a rigid frame and roof supporting vinyl sides. HEPA filters will keep the interior dust-free. These are commercially available products that will be purchased and assembled on-site by U.C. Davis.

A third clean room is planned, perhaps outside the laboratory area, that will house the sources and laser deployment hardware in a clean environment. These will be purchased and assembled at the same time as the gloveboxes.

3.6 Calibration and Monitoring Plan

During the commissioning of each detector, it is assumed that a light flasher will be deployed at the center of the detector for debugging and for adjusting PMT

gains. Once commissioning is complete and detector operation has stabilized, a full calibration program of the detector will be carried out using gamma, neutron, and light flasher sources deployed at representative points in the target and γ-catcher.

After the first full calibration, the process of monitoring begins. The purpose of the monitoring process is to provide the data needed to accurately interpolate detector performance between full calibrations and to help determine when the detector performance has changed to the degree that a full calibration is needed to maintain the required accuracy. On a regular basis (initially at least once per week), a gamma source and a neutron source will be deployed both in the target (along the z-axis using the "fish-line" system) and in the gamma catcher. Once both detectors are operational, monitoring will be carried out on the same schedule for both detectors, with at least one gamma source and one neutron source deployed in both detectors. In addition to monitoring with sources, analyses looking at natural backgrounds will be developed to provide information on detector stability on a day-by-day basis. The frequency of monitoring with sources can be adjusted once the collaboration has experience with the actual stability of the detectors and the irreducible impact of the monitoring process itself on detector stability.

Full calibrations are to be carried out (a) when the detector performance has changed to the degree that monitoring data alone, combined with the previous full calibration, no longer suffice to meet the calibration goals of the detector, (b) after a major change to the detector, or (c) when the maximum interval between full calibrations as set by the collaboration has been reached. To the greatest extent practicable, full calibrations of the near and far detectors will follow the same schedule.

4 Electronics

There are several major tasks that the Double Chooz electronics will perform: (1) providing high voltage (HV) to the PMTs, (2) processing analog PMT signals and delivering them to the Data Acquisition System (DAQ), (3) forming the trigger, and (4) monitoring the detector environment and performance. A subset of the electronics will also be necessary for the PMT initial testing and commissioning. Each of these tasks will be addressed by a combination of commercial and custom-designed electronics. These subsystems will be discussed briefly here, with emphasis given to those items that are proposed to be built by the U.S. DOE groups. A full description of the electronics system as a whole can be found in the Full Collaboration Double Chooz proposal [1], which is available on the web. This proposal requests funds to build the following:

- HV splitter (section 4.2)
- Front-End electronics (section 4.3)
- Slow monitoring (section 4.4)
- PMT rate monitor (section 4.5)

The first two items are similar to the contributions of the U.S. groups to the first CHOOZ experiment, and indeed will be an improved design of that system to be built by the Drexel and Tennessee groups. The last two items are closely related to the calibration of the detector, the other major item of proposed scope. These systems, to be built by the Kansas State and Tennessee groups, will monitor environmental factors that will impact detector efficiency and energy calibration.

4.1 High Voltage System

A quality high voltage (HV) system will be specified and constructed for the near and far detectors of Double Chooz to provide clean, stable, monitored power for the PMTs. The major hardware subcomponents of this system are: a UPS to provide stable AC power, a multi-channel HV supply, and filtering to remove noise.

A single cable will be used for the connection between the PMTs inside the detector and the HV system and Front End Electronics (FEE). Both HV and signal will be carried on the same RG-303 coaxial cable. The FEE includes HV splitters, where signals are picked off the cable. This type of system, which is in wide use, minimizes the amount of cable inside the detector.

The baseline detector design calls for 611 channels of PMT high voltage for each of the near and far detectors. The baseline PMT design requires +2.5 kVDC at 0.1 mA per tube. This can easily be provided by many commercially available power supplies. Selection of a vendor will be made in light of the following specifications:

- *Ripple and noise:* the noise on the HV outputs under load needs to be below a level such that the effect on any signal is less than 0.1 mV peak-to-peak. To meet this requirement, some filtering external to the HV supply will be needed.

- *Voltage set/monitor:* resolution will be at the level of 1 V or better.
- *Voltage limits:* there must be a hardware provision that allows the setting of the maximum output voltage on a module or crate basis. This value shall be read back via software. Software settable controls shall provide the ability to set software limits for the voltage settings.
- *Current trip set/monitor:* resolution must be 1 μA or better.
- *Voltage ramp up/down:* in the range of approximately 10 to 500 V/s, programmable.
- *Operating temperature range:* approximately 0°C to 40°C, dry atmosphere.
- *Grounding:* the HV outputs shall be floating, such that the crate ground is independent of the return for the HV channels.
- *AC power supply:* approximately 220 VAC, 50 Hz.
- *Polarity:* positive polarity modules are required.
- *Communications:* complete control of the HV system must be via a standard TCP/IP Ethernet connection. Provisions to control individual crates from either a front panel or a front panel connection must also be provided.
- *Electrical connections:* the HV connections must be through either standard SHV connectors or an HV certified multi-pin connector of proven reliability in this application.
- *Stability:* 100 mV at a nominal setting of ≈1,600 V for a period of 72 hours.

To date, the three primary candidate-vendors are CAEN, Universal Voltronics and ISEG, all of which have offerings that are potentially acceptable for Double Chooz.

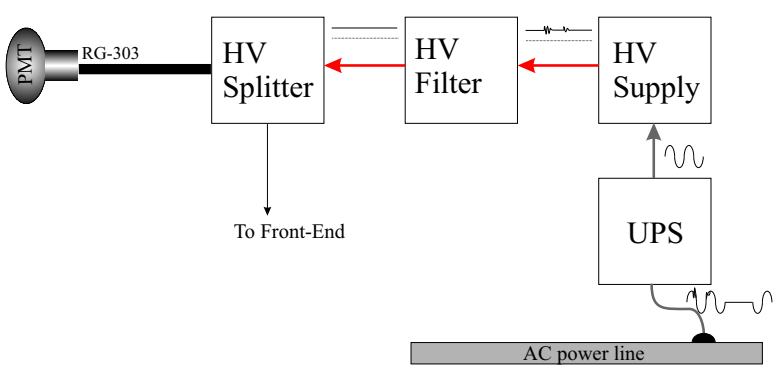

Figure 17: Block diagram of the high voltage (HV) system, showing the major subcomponents.

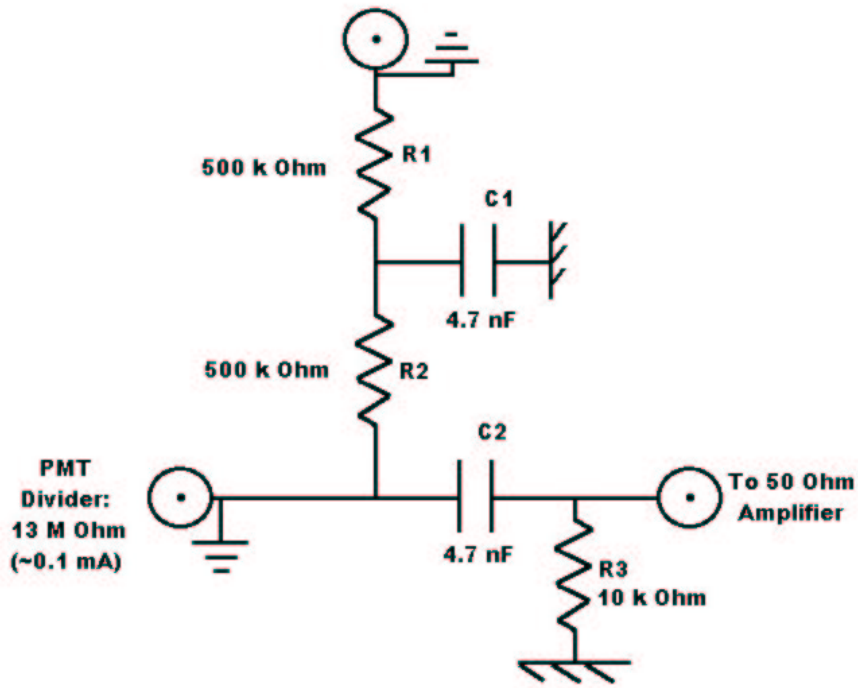

Figure 18: Schematic for the HV splitter prototype. A similar setup was used for the PMT evaluation testing and in a prototype circuit board.

4.2 HV splitter

On their way from the PMTs to the Front-End Electronics, the PMT signals will first pass through HV splitters. Double Chooz will use a single cable for each PMT, carrying both the HV and the PMT signals, in order to minimize cost, dead volume in the detector, feedthrough area at the detector periphery, and ground-loop effects. The PMT signals are expected to be rather small ($\approx$4 mV), so noise must be kept well below the millivolt level.

It is the primary job of the HV splitter to decouple the signals coming out of the PMTs from the HV supplies. In addition, the HV splitters will terminate the PMT cable transmission line to minimize pulse reflections, and provide filtering of the HV to reduce low-frequency noise that comes from the HV power supplies. Figure 18 shows a schematic for a simple four-channel prototype of the HV splitter that has been built. This prototype has the basic features that are expected to be used in the final HV splitter design. Figure 19 shows the simulated performance of the HV splitter with a square-pulse input, a back-terminated PMT, and 100 ns of cable between the PMT and the HV splitter.

For this kind of "RC" termination, required because of the need for HV decoupling, one can expect 3–5% signal reflections. Having termination at both the HV

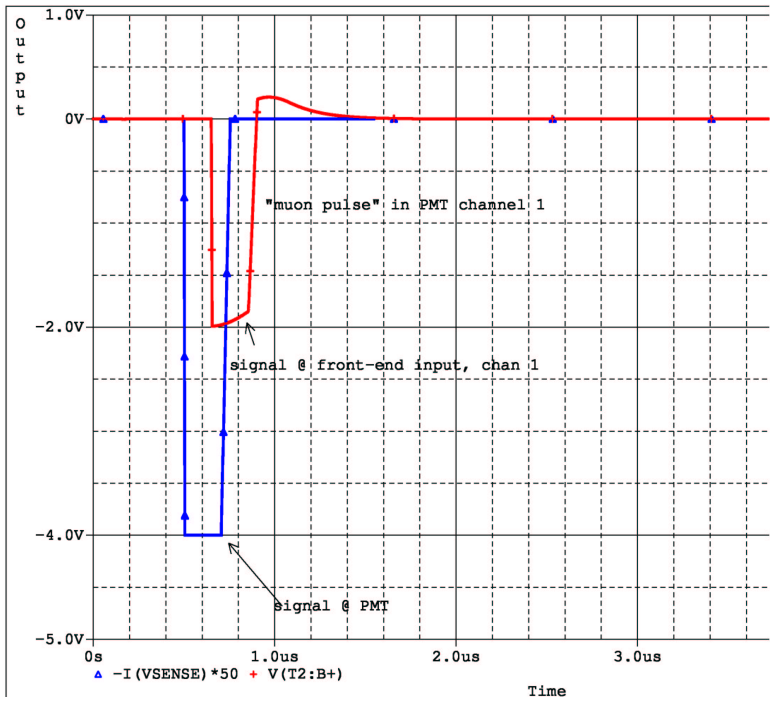

Figure 19: Simulated performance of the HV splitter with a square-pulse input. The use of a square-pulse emphasizes the differentiating effect of the HV blocking capacitance. The factor of two attenuation in overall amplitude is caused by cable termination.

splitter (where the terminating impedance is the output cable) and the PMT base reduces the reflections to well below 1%. An alternative termination scheme, similar to that used on the Borexino experiment [23], was examined and rejected because the presence of parasitic reactances in the the components required the use of significantly smaller decoupling capacitance, with correspondingly larger signal distortion.

Noise from the HV power supply, like ground-loop pickup, would be synchronous across many PMT channels. The summation of the PMT channels to produce energy triggers means that serious attention must be paid to these noise issues.

The series resistors and decoupling capacitor on the HV supply line have the effect of reducing low frequency ($< 1\,\mathrm{MHz}$) noise on the HV supply line to acceptable levels. For one of the HV supplies under consideration the specification for the noise amplitude is 50 mVpp, however the *frequency* of the noise is not specified. Preliminary measurements show that much of this noise is at RF frequencies, and may have to be filtered by a separate HV filter box (not part of the U.S. scope). It is expected that in addition to RF noise, either line noise (50 Hz) or noise from switching power supplies (20–100 kHz) will be present.

Figure 20 shows the measured amplitude at the signal output of the HV splitter from a 50 mV amplitude sine-wave ("noise source") on the HV input, where the resulting output has been multiplied by the number of ID PMT channels to simulate the "worst-case" noise scenario. As can be seen, the result is less than $\approx$1.5 mV,

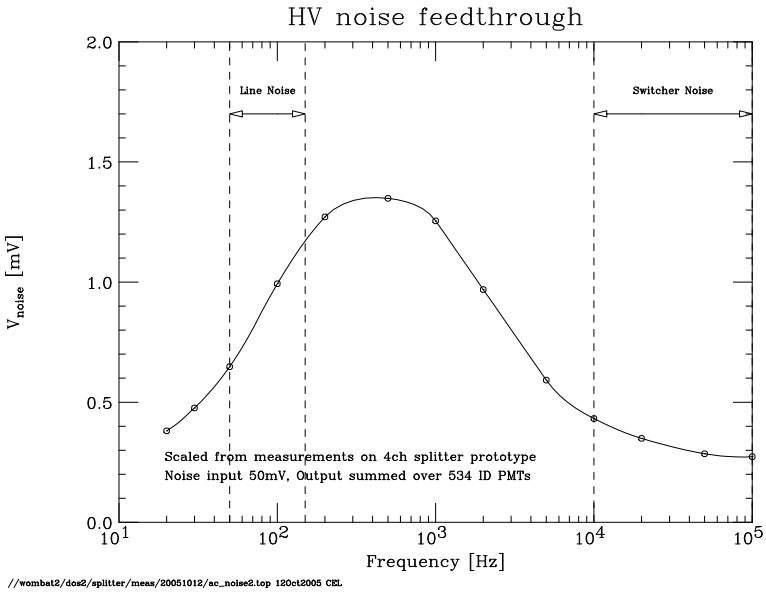

Figure 20: Measured feedthrough of noise on HV supply to PMT signals as a function of noise frequency. The measurements have been scaled to simulate the effect of 50 mV of power supply noise on summed PMT signals. The threshold at which synchronous noise would overcome the level-1 (L1) trigger threshold is approximately 200 mV.

which is considerably less than the ≈200 mV (summed) output expected for a "trigger threshold" event.

Another concern is the possibility of cross-talk between the channels. In a detector of the Double Chooz design, one expects cross-talk not to be a serious concern: all of the PMTs are looking at the same events, and should have similar signals. There simply won't be cases of valid events where one PMT gets a large (muon-like) signal, while an adjacent PMT only gets single photoelectrons. However, the simulation of the HV splitter shows essentially zero cross-talk ($<50\,\mu$V for a 4 V input pulse) between channels.

One can still have capacitively or inductively coupled cross-talk between channels that is not apparent in the simulation. Tests will be conducted at every stage of the HV splitter (and other downstream electronics) to measure, and if necessary mitigate, any cross-talk.

Integration with monitoring systems The Slow Monitor (see section 4.4) is not expected to have temperature or voltage monitors located on the HV splitter circuit boards, because of the complications of isolating the low-voltage monitoring system from the high voltages nearby. However, it is planned to have several temperature sensors inside each HV splitter enclosure, with the sensors connected to the slow-control monitoring bus.

Stability, temperature and humidity The plan is for the HV splitters to be located in the detector hall, on the walls to the side of the detector. The proximity to the detector reduces the length of expensive RG-303 cable needed.

This location is outside of the air-conditioned room used for most of the other electronics, and subject to more variation in temperature and a potentially higher humidity. Both of these environmental issues are addressed in the mechanical and electronic design of the HV splitter.

High voltage capacitors are subject to variation in their capacitance with temperature and applied voltage. For the capacitors used for noise filtering and DC stability, the exact value of their capacitance is not important so long as they are sufficiently large. However, the decoupling capacitor in the signal path has a direct effect on the PMT pulse shape received by the Front-End electronics.

For these critical capacitors, the HV splitter design calls for the use of C0G-type dielectric, which exhibits no change of capacitance with applied voltage and a temperature coefficient of less than 30 ppm/°C.

Similarly, series resistors in the path between the HV supply and the PMTs need to have sufficiently small temperature coefficients so that the voltage supplied to the PMTs does not vary significantly as a result of temperature changes in the HV splitter enclosures. Standard resistors have temperature coefficients of 100 ppm/°C, which would result in less than 1 V change in PMT voltage with a 10° C change in temperature. Resistors with smaller temperature coefficients are easily obtained, if necessary.

The humidity in the laboratories (outside of the electronics room) may be close to 100%, which is potentially a problem for HV electronics such as the HV splitter. Two approaches are being pursued to minimize possible problems with humidity in the HV splitter. Any components that are sensitive to humidity, including connections to the printed circuit board where discharges could occur, will be coated with a conformal coating, silicon compound, or epoxy. This type of encapsulation is also desirable from a safety standpoint. The application technique (known as "glob-top") has been tried on prototype HV splitter boards and looks practical, although there has not yet been testing to measure HV leakage, humidity effects, etc. In addition, provisions will be made to supply dry air (at a low, constant rate) to the HV splitter enclosures.

Cabling Cables from the HV power supply to the HV splitters will be provided (not in the U.S. scope). The type and quantity of the cables from the HV supply will be determined after the vendor is selected, as they may use different connector/cable types.

4.3 Front-End Electronics

The Front-End subsystem receives PMT signals from the HV splitter, performs amplification, pulse-shape and baseline corrections, and distributes the signals to downstream electronics (see Fig. 21). The input signals to the Front-End will be quite small (millivolt level), so the entire Front-End will be a purely analog design to avoid

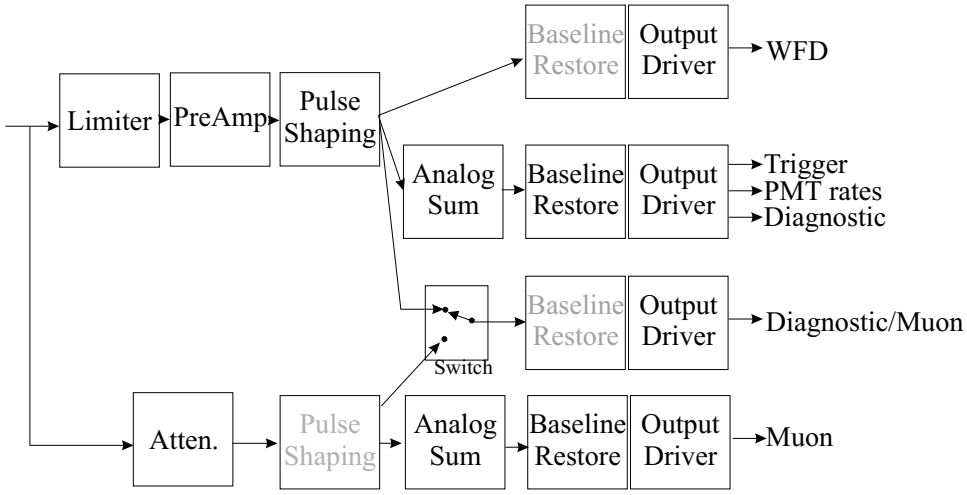

Figure 21: Block diagram of Double Chooz analog Front-End functions. This design will also be used for performing analog summation for the L1 trigger. The "switch" in the diagram will be implemented with a zero-ohm surface-mount jumper. The channel-disable and calibration input functions are not shown in this diagram.

any digital noise leaking into the signals. Wherever possible, the electronics is kept simple and linear so that we can easily reconstruct the effect of the electronics on the signals. Ample diagnostic and calibration capabilities are being designed into the system. The idea is that the electronics doesn't just need to work, but we need to be able to demonstrate that it works as expected throughout the lifetime of the experiment.

The implementation plan is to first test and optimize individual functions of the Front-End (summation, baseline restoration, etc.) using specific prototype circuit boards, then to produce a "few channel" prototype that includes the full range of circuitry for a limited number of channels, before proceeding to a final design of the Front-End module.

This plan of creating small, cheap prototypes of simple functions has been pursued for the past two years with several small full-speed PCB prototypes (see Fig. 22 for an example), a number of reduced-speed prototypes to verify overall circuit concept, and extensive SPICE simulation which is compared to prototype results.

Amplification: Current-feedback amplifiers will be used to provide gain in the Front-End modules, and as output drivers. These amplifiers have excellent stable high-frequency performance with the large slew-rate needed for fast PMT signals (see Fig. 23) The total gain required is in the range of 10–15, so that single photoelectron signals ($\approx$ 2 mV) are at an appropriate amplitude (20–30 mV) for the Wave Form Digitizer (WFD) system. The gain will be manually adjustable (within a reasonable range) to allow accurate performance matching between channels.

Selecting amplifiers for good performance in bandwidth and noise generally means sacrificing DC accuracy. Baseline restoration is thus required and is discussed below.

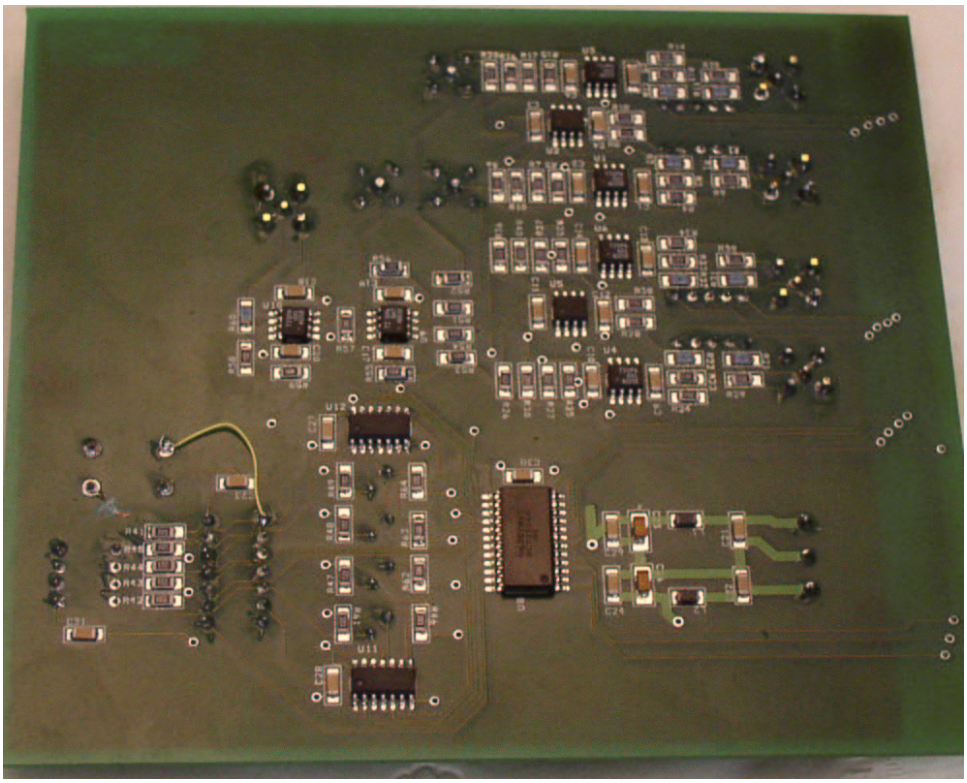

Figure 22: Photograph of a recent prototype circuit board for testing some Front-End functions. These small prototypes are designed and completed on a timescale of approximately one month.

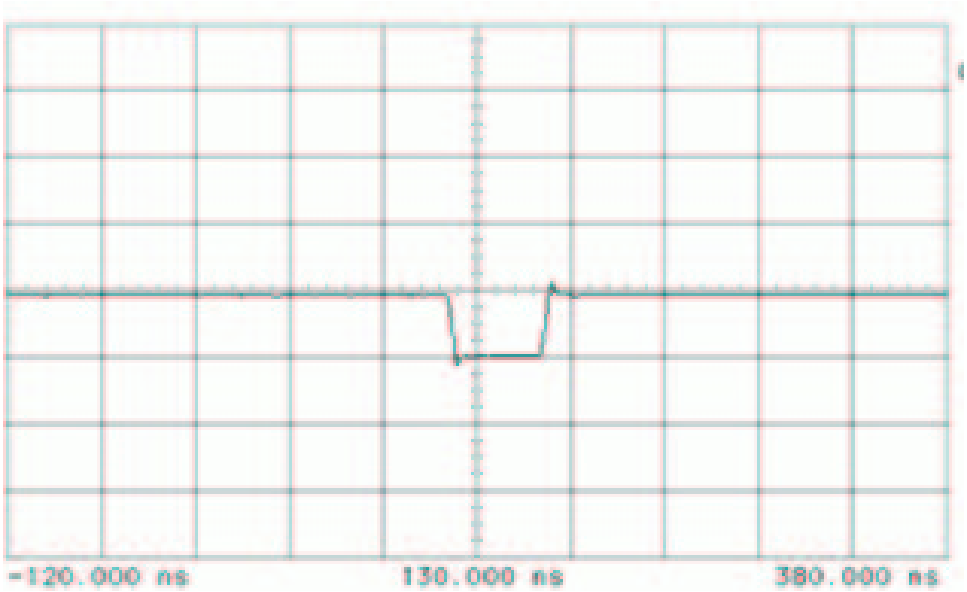

Figure 23: Oscilloscope trace from the output of a prototype Front-End amplifier, where a square pulse was applied at the input. The vertical scale is 500 mV/division. The amount of pulse distortion is clearly quite small.

Several prototype amplifier circuits have been built, with good performance. The design of the basic amplification part of the Front-End is well developed.

Calibration input: There will be a single calibration input per Front-End module that allows the introduction of calibration pulses to the Front-End channels. When combined with the channel disable capability, this allows the calibration input to be routed to a selected subset of Front-End channels.

Pulse shaping: It is planned to have some simple pulse shaping in the Front-End modules to reduce the effects of cable attenuation and pulse distortion from HV decoupling capacitors.

Baseline restoration: We will avoid some of the baseline-shift problems caused by large (muon) signals and capacitive coupling by using DC coupled circuitry wherever possible. As mentioned previously, however, the high-speed amplifiers needed tend to have unacceptably large DC offsets. The baseline restoration circuitry will apply low-frequency corrections to cancel the offsets and improve the rejection for low-frequency pick-up.

Two prototypes using different techniques of baseline restoration have been built and tested. Both have been successful, and further evaluation and testing is underway to decide on a final scheme. Figure 24 shows the schematic of the second of the two baseline restoration prototype circuits, with the associated channel disable relay.

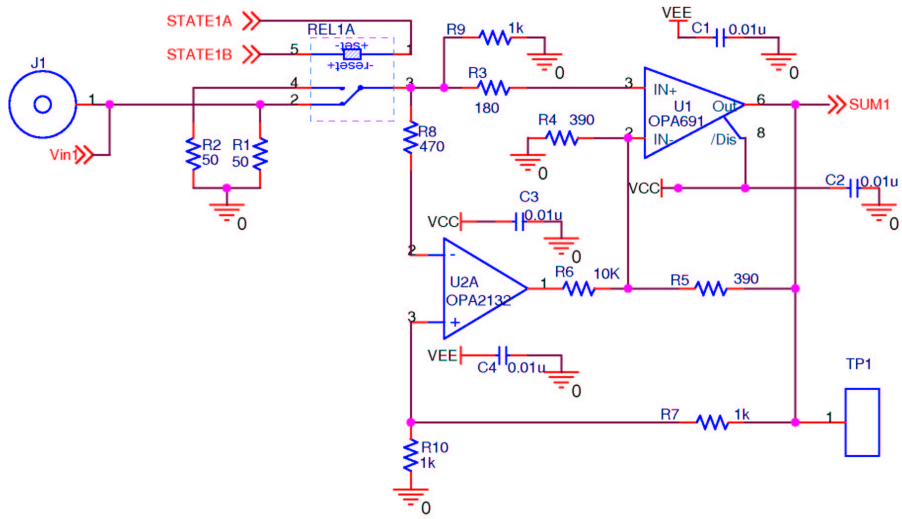

Figure 24: Schematic for the second baseline restoration prototype, including a channel-disable relay on the input. The relay is bistable, so that the relay coil is only energized to change the state of the relay. This particular circuit uses a precise low-speed amplifier to correct the low-frequency performance of the current-feedback high-speed amplifier.

Pulse summation: A linear analog sum of the input pulses will provide signals for the L1 trigger, rate monitoring, and diagnostics. There are two candidate circuits that look promising for performing the summation.

A prototype that included pulse summation was built but exhibited oscillation in the summation stage as a result of using a fast voltage-feedback oscillator with some parasitic capacitance. Additional prototype tests are needed to try different summation circuits and layouts. A board will soon be finalized.

Muon/Trigger channel: A separate attenuated path through the Front-End will be provided for use in further stages of analog summation (in separate modules) or for an attenuated "muon channel" (in the Front-End modules). The attenuation helps to avoid any electronic limitation of muon singles, but at the expense of low-amplitude signal information. We will have the option (via zero-ohm surface mount jumpers) of having individual muon outputs for each input, or of having only a summed muon output.

ΣQ Trigger Detectors in which an inner scintillator volume is surrounded by PMTs distributed uniformly have the property that the total amount of light collected by the PMTs is directly proportional to the energy deposition if the effects of light attenuation are small. For Double Chooz the distribution of PMTs is not perfectly uniform, however, it is close enough to uniform to make total light a useful proxy for event energy. In addition, the small size of Double Chooz makes light attenuation

only a small correction, negligible for the purposes of creating a trigger.

As a result, a simple *energy* trigger for Double Chooz is simply to sum up the PMT signals from the inner detector and use a discriminator to set an energy level for the trigger. The ΣQ trigger is based on the analog sum of PMT signals to determine the energy deposition.

In practice, the summation of so many PMTs means that any common-mode noise (ground-loop noise, etc.) has to be suppressed since such noise sources would be amplified in the summation. This motivates much of the efforts in upstream electronics systems to avoid or ameliorate noise inputs.

ΣQ modules: The trigger summation occurs in several stages; the first stage is in the Front-End modules, where all of the input signals handled by that module are summed and provided on an output. Additional levels of summation are required, which will be provided by ΣQ modules. The ΣQ modules take a set of inputs and provide an attenuated and summed output. This is exactly the same functionality provided in the Front-End for handling muon signals and is very similar to the general functionality of the Front-End modules. Rather than having two separate designs for Front-End and ΣQ modules, we will use a single design that can be used (with minor changes) for both functions. The ΣQ modules will be Front-End modules with only those components that are necessary for their function. This will simplify the design process and also be quite cost-effective. We will also be able to make use of the channel-disable and calibration input functionality in the ΣQ modules, if these are needed for calibration and testing purposes. Outputs from each stage of summation will be made available to monitoring systems to check stability.

ΣQ Pulse stretching Light from a point-like event in the detector arrives at the PMTs at different times, depending on the position of the event. As a result, when summing pulses to determine the energy of an event, pulse timing effects can result in a summed pulse that is smaller than it should be. This has the effect of producing a position-dependent energy threshold. We need to minimize the position-dependence of our ΣQ energy threshold by stretching the trigger pulses to minimize time mismatch effects. One approach to this problem is to use a simple integrator (or RC circuit). The difficulty with this approach is that the RC "droop" after an early pulse still results in the output pulse being affected by pulse timing mismatch. This can be improved by increasing the integration time, but only at the expense of increasing the accidental trigger rate when unrelated sub-threshold events are summed.

Figure 25 shows a possible approach to pulse stretching that is linear and introduces no dead-time, unlike discriminator-based linear stretchers. The input pulse and a delayed, inverted copy of the input pulse are summed in an integrator. The width of the resulting output is primarily determined by the delay line, while the integrator time-constant should be sufficiently long to make the output pulse reasonably flat. The SPICE simulation of this circuit is shown in Fig. 26.

This circuit has been tested in a simple prototype (see Fig. 27), and shows the

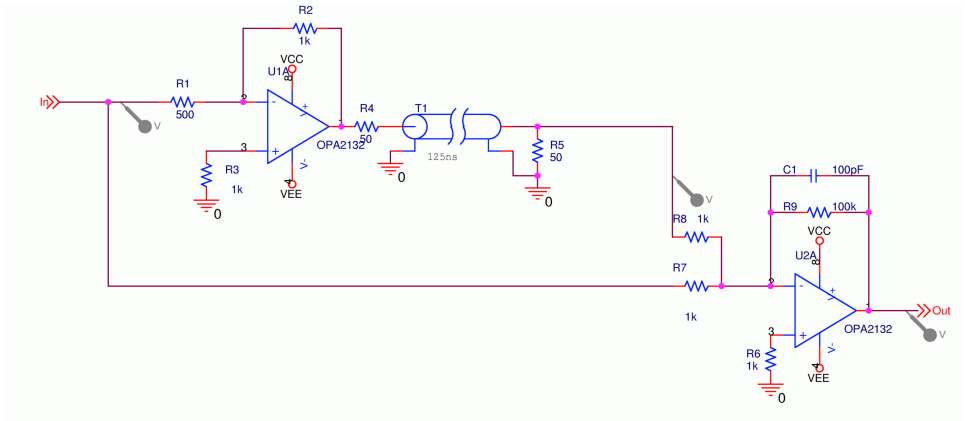

Figure 25: Schematic for an early prototype ΣQ trigger pulse stretcher that was simulated and tested. The input pulse is stretched by a length of time determined by the delay-line.

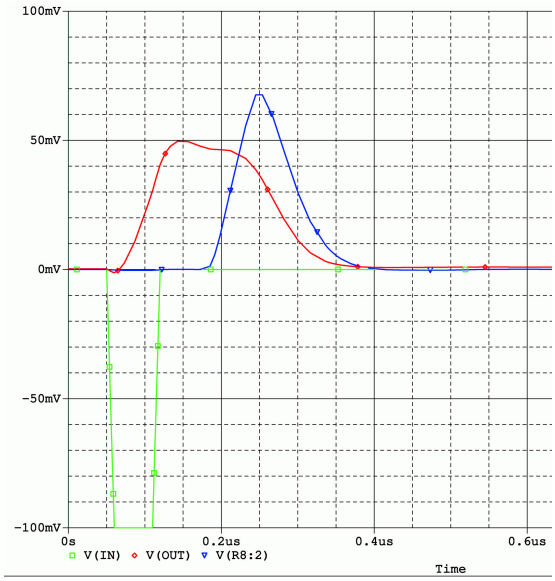

Figure 26: SPICE simulated response of the ΣQ trigger pulse stretcher. The input pulse is the leftmost large negative (green) waveform, the output of the delay line is the rightmost (blue) positive pulse, and the output of the stretcher is the positive (red) pulse in the middle. While the output pulse exhibits some bumpiness, it is much flatter than an exponential of similar width.

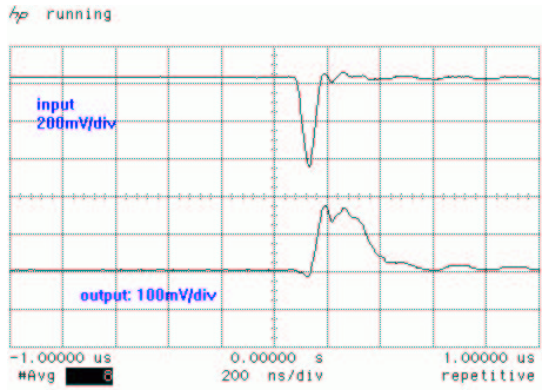

Figure 27: Waveform capture from an early prototype ΣQ circuit (top trace is input, bottom trace is output). This prototype shows that the general scheme for stretching ΣQ pulses works, although the prototype operated at lower speed (and with more parasitics) than what one needs for the final design.

general features expected from the simulation; however, testing of a more complete full-speed prototype is needed to determine the suitability of this circuit for Double Chooz.

The trigger and timing system must provide a highly efficient trigger to the Double Chooz experiment for neutrino events as well as for several types of background events. The trigger has to be reliable, *i.e.,* trigger failures must be rare and easily detectable, and the trigger efficiency must be measurable with sub-percent precision. The trigger system will also distribute a common clock signal to the experiment and provide a time stamp for all events.

There will be a two-stage trigger system. The level-1 trigger is based on the analog ΣQ signals from the detector which are discriminated and analyzed in FPGAs (Field-Programmable Gate Arrays). A positive level-1 decision triggers the readout of the detector. The readout is followed by a level-2 software trigger. It rejects further events before the data are written to tape. This section covers the level-1 trigger only.

There will be independent trigger systems for the far and near detector with independent clocks. The frequency of the clocks in both detectors must be identical. The clocks will be synchronized between the two detectors through either a cable connecting the two triggers or through GPS systems. Synchronization of the phase is not required.

The trigger will receive input from the PMTs of the inner detector and the inner veto from the ΣQ analog sums (see Section 4.3). The trigger receives only the signal sums. Inputs from the outer veto and the calibration systems can also be processed (for example from the laser system, section 3.3). It is possible to apply veto conditions at the trigger level, but this is not foreseen. Instead, an event in the veto detectors will be read out as well as a neutrino candidate following it. It is left to the offline analysis to reject cosmogenic events. The signals of the groups of

PMTs are discriminated individually to provide an approximate multiplicity of the event. In parallel the total signal sums from the inner detector and inner veto are derived and discriminated on several levels. The trigger will thus allow conditions on the total energy and multiplicity, or any combination of these, to be applied.

To keep the trigger conditions flexible, FPGAs will be used to apply the trigger conditions to the discriminated signals. For redundancy, two independent trigger boards will be used for the inner detector, each based on only half of the groups of PMTs. This guarantees that hardware failures do not cause loss of events and can be easily detected. A third trigger board will handle the inner veto and additional trigger inputs. A careful simulation will determine the initial trigger conditions. They can be adapted once experience with the real detector is available. The following list gives initial ideas on some of the necessary trigger conditions:

- **Inner Detector Neutrino Trigger A**
  Approximately 0.5 MeV energy threshold on the total energy in the inner detector and at least 2 groups of PMTs above noise (to exclude single sparking PMTs from triggering). The trigger is based on the first half of PMTs only (groups A).

- **Inner Detector Neutrino Trigger B**
  Same as above, but based on the second half of PMTs (groups B).

- **Low Energy Neutrino Trigger A + B**
  This trigger is the same as above, but with a lower energy threshold. Its rate will be too high and therefore only a prescaled selection of events will create a real trigger. The energy threshold and the prescale factor will be adjusted based on the detector noise level. This trigger allows the threshold behavior of the main neutrino trigger to be studied.

- **Inner Detector Muon Trigger A + B**
  A muon will create a signal in the inner detector that fires all groups of PMTs. The trigger will be based on multiplicity only.

- **Inner Detector Muon Trigger A + B (PMTs with low gains)**
  Some PMTs set with a low gain could be installed to better detect and tag showering muons.

- **Inner Veto Muon Trigger**
  A trigger based on energy threshold and minimum multiplicity in the inner veto.

- **Inner Veto Low Energy**
  A trigger on the inner veto with a lower threshold to study the trigger efficiencies. Scaled down in rate as above.

- **Random Trigger**
  A trigger with an adjustable frequency triggering the readout at fixed time intervals. The events will allow detector noise to be studied.

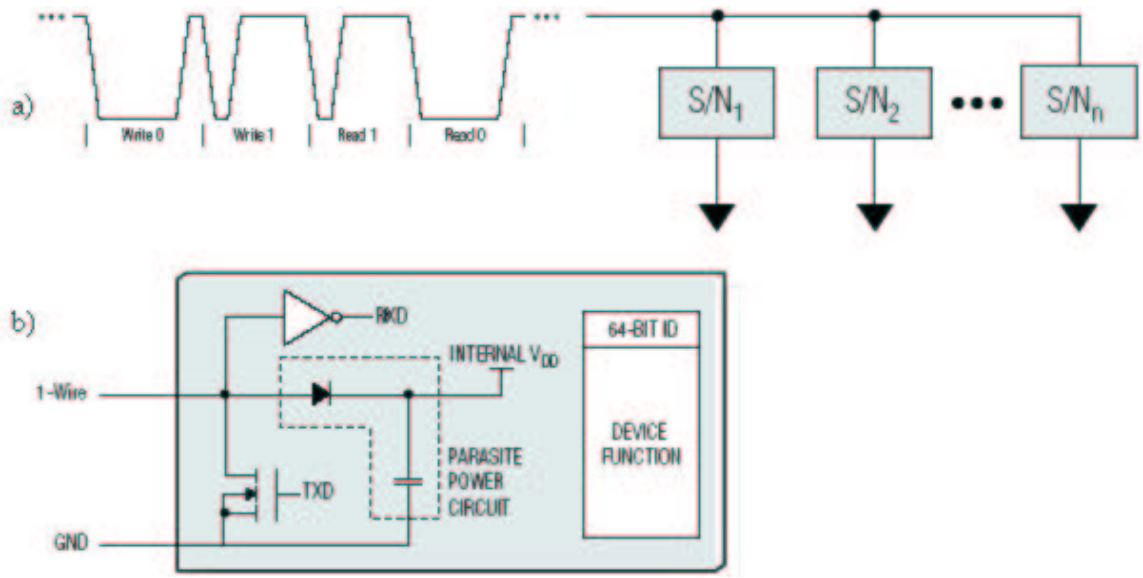

Figure 28: The 1-Wire® bus: (a) control, readback, and power provided to multiple devices over a "single" wire; (b) parasite power circuit captures power during high period of 1-Wire® waveform. (Adapted from figures by Maxim IC/Dallas Semiconductor.)

4.4 Slow Monitoring

A slow monitoring and control system is required in order to control systematic effects that could impact the experiment, to allow automated scans of parameters such as thresholds and high voltages, and to provide alarms, warnings, and diagnostic information to the experiment operators. The quantities to be monitored and controlled include temperatures and voltages in electronics, experimental hall environmental conditions, line voltages, liquid levels and temperatures, gas system pressures, radon concentrations, phototube high voltages, and discriminator settings and rates. Most of these functions can be accomplished using "1-Wire®" devices from Dallas Semiconductor [25]. The high voltage and discriminator subsystems will have their own control and readback hardware. All slow monitoring and control systems will use the same database and history log software. A computer in each experimental hall will monitor the local 1-wire bus and a local radon monitor, acquire any data provided by other subsystems, record the data, and make the data available via the local internet connection.

Monitoring via 1-Wire interface The "1-Wire®" line of semiconductors from Maxim IC / Dallas Semiconductor use a simple interface bus that supplies control, readback, and power to an arbitrary number of devices over a single twisted-pair connection [25], as shown in Figure 28. A variety of sensor and control functions are available in traditional IC packages and stainless-steel-clad "iButton®s,"; two examples are shown in Figure 29. Each device has a unique, factory-lasered and

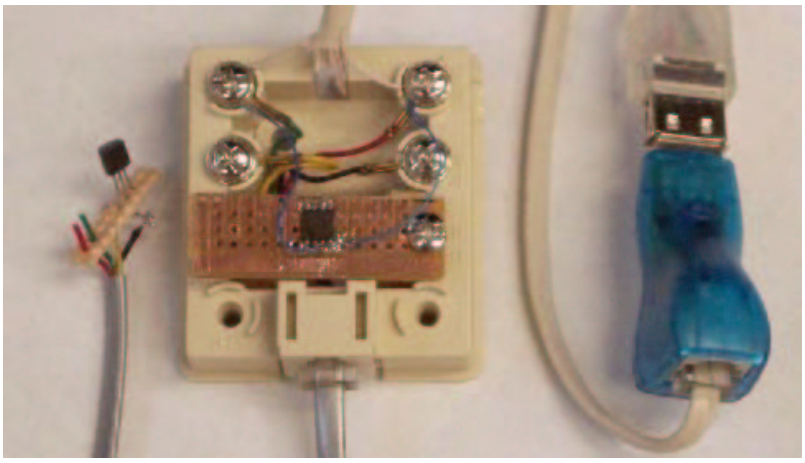

Figure 29: Examples of 1-Wire devices. From left to right: digital thermometer in TO-92 package; 4-channel ADC on prototype board, mounted in RJ-11 modular phone jack box; USB to 1-Wire interface.

tested 64-bit registration number used to provide device identification on the bus and to assure device traceability. Some devices are available in individually calibrated NIST-traceable packages. The features of low cost, capability to connect all devices to the same set of wires in parallel, unmistakable device ID, and versatility make this an attractive choice for implementing the slow instrumentation and control system. Implementation details and expected performance for several subsystems are given here.

Crate and card temperatures and voltages: Temperature and voltage monitoring can be included in any custom-built electronics at a component cost of only a few dollars per device using DS18S20 and DS2450 chips and low-cost modular connectors to connect to the 1-Wire® bus. Note that in addition to the temperature and voltage functions, the unique ID on each chip provides automatic tracking of any card swaps. Trivial custom boards containing only these components can be used to monitor temperature and bus voltages on crates which otherwise contain no custom-built electronics.

In these chips, digitization of temperature and voltage is initiated by an explicit "convert" command from the bus master. Temperature conversion takes 900 ms, and digitization of the four 12-bit channels of the DS2450 takes less than 4 ms total. During conversion, the bus master may communicate with other devices if the chips have an external source of power; if a chip is powered parasitically from the bus, then the master must maintain the bus level high throughout the conversion. Testing of samples provided by Maxim IC/Dallas Semiconductor confirm that multiple devices can maintain their internal state while all are powered parasitically from the same bus. Figure 30 shows data from a three day period during which two DS18S20 thermometers were sampled once a second by a program written in Java. The two thermometer chips were mounted in direct contact with each other, and recorded

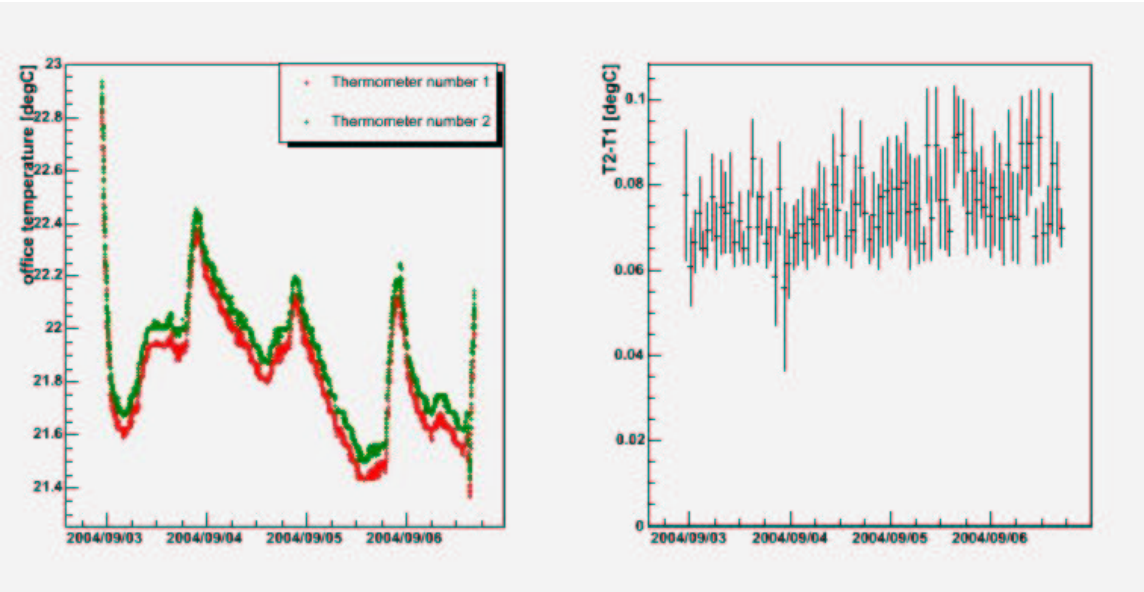

Figure 30: Data from three day test of several 1-Wire® samples: (a) temperature in an office at Kansas State University vs. time as read by two adjacent DS18S20 thermometer chips; (b) difference in reading of the two chips.

the same temperature to within a small fraction of a degree. In this test, the thermometers were located about two meters from the bus master, and another 1-Wire® device was connected on the same bus about three meters further downstream. No failures or interruptions occurred during this period.

Experimental hall environment: The DS1923 "Hygrochron" iButton® looks ideal for monitoring temperature and humidity. In addition to the humidity and temperature functions, this device features on-board battery backup and automatic logging to internal memory independent of external control. Power or computer failures will not interrupt the temperature and humidity record. This iButton® is designed for tracking sensitive products during shipment or other handling. Each DS1923 is individually calibrated and NIST traceable. Another iButton®, the DS1922, provides similar functionality without the humidity function.

Monitoring of barometric pressure and other environmental factors is easily achieved using the DS2450 ADC and one or more external transducers. (Note: A complete 1-Wire® weather station is also available [26].) Another interesting "environmental" condition to monitor is ambient light level in the experimental area: many systematic effects in past and present neutrino experiments have been attributed, correctly or incorrectly, to electrical or optical noise introduced by lighting, and a simple phototransistor addresses the issue handily. The phototransistor technique also can be used to monitor status LEDs on devices which lack electrical status outputs. AC line voltage is also easily monitored using a 1-Wire® ADC and a trivial circuit.

Liquid levels and temperatures, and gas pressures: Transducers will be provided for monitoring important aspects of the detector such as scintillator and buffer oil levels, temperatures, and pressures in any gas systems used. Transducers should produce voltages in the 0 to 5 V range for maximum compatibility with the DS2450 ADC. The further specification, purchase, and installation of such transducers are the responsibility of the respective subsystem providers.

Simple controls: The DS2890 is a 1-Wire® digitally controlled potentiometer. It can be used to provide slow control for simple servos, power supplies, or other devices controllable by an external analog signal. At present, there is no definite plan to use this capability, although the discriminator levels could possibly be controlled in this way. Support for slow control as well as monitoring will be provided in the software for maximum flexibility.

Radon monitoring Commercial continuous radon monitors have become readily available and relatively inexpensive. An example is Sun Nuclear's Model 1027 [27]. Each experimental hall will have at least one radon monitor read out by the slow control PC. The data will be stored and made available via the same interface used for all slow monitor data.

Magnetic field monitoring The Double Chooz photomultiplier working group has identified a need to monitor the magnetic field in each detector at multiple locations. Slow remagnetization of the individually degaussed iron bars in the iron shield could lead to localized magnetic fields sufficient to affect the performance of photomultipliers in one region of the detector. Since phototube performance can be affected by more than one factor, monitoring the magnetic fields is important to understanding the performance of the detector. Readily available and inexpensive three-axis magnetometers, such as the Honeywell HMC2003 [28], can be easily interfaced to 1-Wire® ADCs, as demonstrated by prototypes constructed and tested at Kansas State University. A dozen such magnetometers per detector will provide sufficient coverage.

Interface to other subsystems Some hardware subsystems may have important slow monitor data that cannot be made available on the 1-Wire® interface or the serial ports of the slow monitor computers. Examples may include the clean room particle counters, the high voltage power supplies, and the discriminator circuitry in the trigger system. In such a case, either the hardware itself or a computer which monitors and controls it should make the data available via network TCP connection. "Virtual" monitor data, such as capture time, event rates, or other quantities determined by online analysis, could also be recorded by this mechanism. The software on the master slow monitor computers will poll these external servers and make all slow monitor data available in a common framework. This is preferable to each subsystem providing a separate data interface. In the common framework, systematic correlations may be studied among any variables. Support for control

functions and synchronization with externally controlled devices should be provided in the software to allow for scans of controlled parameters such as high voltages and threshold levels. The common framework will allow dependent variables observed in one subsystem, *e.g.*, discriminator rates, to be easily correlated with parameters monitored or controlled by some other subsystem, *e.g.*, high voltage.

4.5 PMT Rate Monitor

The stability of the Double Chooz detectors is of great importance to the overall physics result of the experiment. Indeed, it is necessary that the detectors be stable over time (after calibration) to better than 0.5%. Stability at that level cannot be assumed and needs to be subject to constant verification.

One of the most sensitive indications of stability for a scintillation detector is the rate of single photoelectrons from the PMTs. This rate is highly sensitive to changes in the PMT gain (whether caused by high voltage, magnetic fields, PMT aging or other effects), the scintillator efficiency and light attenuation, and changes in the electronics. If the single photoelectron rate is stable, it gives confidence that many critical parts of the detector are also stable.

The PMT Rate Monitor for Double Chooz can be implemented very simply with a handful of commercial VME modules. Figure 31 shows a possible implementation using standard CAEN modules.

While it may be desirable to monitor individual PMT rates, the stability of the detectors can also be monitored by using fanned-in PMT signals with minimal loss of sensitivity, but with a significant decrease in cost (and in Front-End connector space, which is very limited). The current plan is to use 16:1 fanned-in PMT signals from the Front End electronics. Each of these signals then goes to an input of a 16 channel VME discriminator, requiring only 4 discriminator modules to fully cover one Double Chooz detector. The outputs of the discriminators then are connected (by ECL twisted-pair ribbon cable) to a pair of 32 channel VME scalers, which have channel-scanning readout and buffered memory capabilities. With these (or similar) modules, each monitored channel can be counted for a fixed length of time on a 32-bit scaler, and result stored for later asynchronous readout.

As an example, assume that each PMT has a singles rate of approximately 5 kHz. With 16 PMTs summed together, that gives 80 kHz per rate monitor channel. Using Poisson statistics, a 1% jump in the rate from a single PMT would be detectable as a 9σ deviation with forty five minutes of rate monitor data. Over a longer period of time, drifts in singles rates can be measured with outstanding accuracy.

During the commissioning of the detectors, and for debugging purposes, it is very useful to be able to measure PMT singles rates from individual PMTs. This capability is made available by using the "channel-disable" feature of the Front-End electronics. In addition, it will be possible to vary the discrimination thresholds via VME to understand the PMT signals in considerable detail.

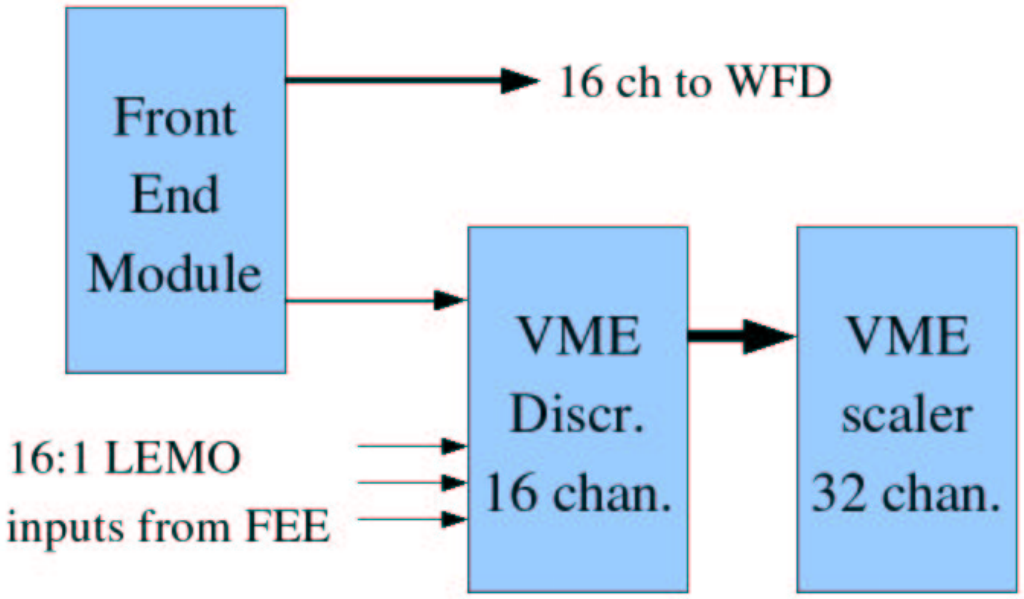

Figure 31: Schematic of a PMT Rate Monitor implemented with CAEN V.814 discriminators and V.830 latching scaler modules.

	K-40, ppb	Th, ppb	U, ppb
Target	0.000001	0.000001	0.000001
Acrylic	0.01	0.01	0.01
PMT	23.9	164	66.4
Catcher	0.000001	0.000001	0.000001
Buffer	0.000001	0.000001	0.000001
Veto	0.000001	0.000001	0.000001
Steel	0.54	3.3	2.3
Rock	1638	5000	2000

Table 14: Activities used for calculation of singles rates.

5 Radiopurity Assessment

5.1 Comparison with Chooz

The Chooz detector had a background singles rate of around 130 Hz, which became 65 Hz above 1.3 MeV after all data cuts. Coupled with a "neutron-like" event rate of 45 Hz, this meant that about 30% of the correlated background measured by Chooz was due to random coincidences. We wish to improve upon that number for Double Chooz, even though we have a larger detector by a factor of two.

To this end, we have designed a shielding plan that improves the singles rate in the target by more than an order of magnitude while using the same size detector cavity. A calculation of the singles rates in Chooz and Double Chooz is shown in Figure 32. This plot is based on an analytical model designed to calculate the rate of single gamma hits for detectors with complex multi-layer geometries. The model was validated against the KamLAND detector, where single rates are known very well. Radioactive contaminant activities used for this model are given in Table 14. They are typical values and not difficult to achieve with reasonable care.

Figure 32 shows the gamma ray interaction rate per unit volume starting from the surrounding rock for both CHOOZ and Double Chooz detectors. The largest difference comes from replacing the sand used in CHOOZ with a steel shield, which attenuates the gamma rays entering the detector from the surrounding rock considerably. Note also that a mineral oil buffer has been added between the PMTs and the target to attenuate gamma rays originating in the PMT glass. As a result, the predicted activity per unit volume is about two orders of magnitude lower in Double Chooz than for CHOOZ.

5.2 Activity of Materials

Detector Materials A survey of the literature has been done to get an idea of the radiopurity levels available in the materials to be used in Double Chooz. Representative values for detector materials are presented in Table 15. These data do not represent the total survey sample, but are included to show what variations have

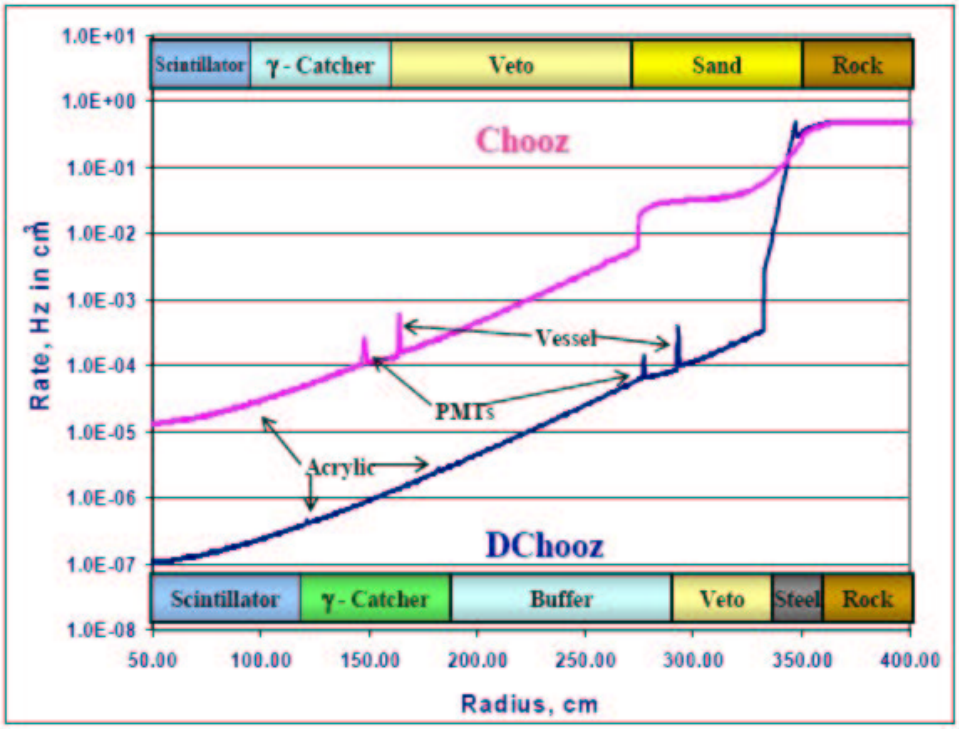

Figure 32: Comparison of the predicted singles rates in CHOOZ and Double Chooz. The figure illustrates a simple model where both Chooz and Double Chooz are considered to be spherical instead of cylindrical. This model accounts for the generation, propagation, and attenuation of gamma rays through each layer, using appropriate activities and attenuation coefficients for 1 MeV gamma rays. The main differences between Chooz and Double Chooz arise from the addition of a nonscintillating buffer close to the PMTs and the replacement of 70 cm of sand by 17 cm of steel to better shield the detector from external gamma rays.

source	K(ppm)	Th(ppb)	U(ppb)
Steel			
KamLAND	1.88	0.7	0.7
KamLAND	0.85	0.7	0.3
SNO	10.	14.	5.0
Acrylic			
KamLAND	0.07	0.05	0.008
SNO		0.008	0.004
CHOOZ	0.00012	0.001	0.001
Chooz Rock			
CHOOZ	2000.	5000.	14000.

Table 15: Typical activities of various materials from a literature search.

source	K(ppm)	Th(ppb)	U(ppb)
ETL, glass, manufacturer	60	30	30
ETL, glass, Alabama	100 ± 16	36 ± 7	21 ± 9
ETL, glass, MPIK	59	156	54
Hamamatsu, glass, Alabama	204 ± 22	164 ± 24	66 ± 11
Photonis, glass, LBNL	110 ± 10	65 ± 6	180 ± 10

Table 16: Measurements of PMT radiopurity.

been seen.

Cobalt-60 is also a radioactive component of some steels, so the activity of such material used in the detector must also be considered. For example, the stainless steel buffer tank will be required to have a cobalt-60 activity less than 10 mBq/kg.

Photomultipliers Since the borosilicate glass of photomultipliers can contain radioimpurities (^{40}K, ^{232}Th, ^{238}U) and the photomultipliers are positioned close to the scintillator volume, particular care must be given to the selection of PMTs with low concentration of radioimpurities in the glass. Three leading PMT manufacturers (ETL, Hamamatsu, and Photonis/Burle) provided us with samples of low-radioactivity PMT glass. Radioassay of these samples was made at the low-counting facility at the University of Alabama, at MPI/Heidelberg, and at LBNL. The results of these measurements are shown in Table 16. Radiopurity data for PMT glass from ETL and Hamamatsu are generally confirmed by our radioassay measurements, although there are some discrepancies between measurements performed by different groups. It is also possible to have tube to tube variations. We currently plan to test non-destructively several PMTs from ETL, Hamamatsu, and Photonis to verify and extend these results. The current measurements, when input into our U/Th/K/Co event generator and detector simulation, result in a background singles rate less than 10 Hz at a threshold of 0.7 MeV. This rate would result in less than 2

component	High > 0.5 MeV	High > 1.0 MeV	Low > 0.5 MeV	Low > 1.0 MeV
PMT	5.0	2.9	2.1	1.2
target tank	0.11	0.085	0.0034	0.0029
GC tank	0.17	0.12	0.0062	0.0037
buffer tank	1.8	0.93	0.67	0.25
veto and shield	1.7	1.0	0.11	0.063
Chooz rock	1.4	0.86	1.4	0.86
total	10.	5.9	4.3	2.4

Table 17: Expected rate (Hz) of single gammas above 0.5 and 1.0 MeV interacting in the scintillator. These results are based on a GEANT3 simulation using the material activities given above, with high and low indicating the activity value used for the simulation.

events/day above 1 MeV in our far detector, which can be accurately subtracted and is acceptable. Thus, the manufacturers are capable of producing PMTs of sufficient radiopurity for our purposes. It is our intent, however, to include radiopurity in the PMT specifications, and to perform non-destructive counting on a random sample of delivered PMTs to ensure radiopurity quality and consistency. A new low-counting facility will be built at U.C. Davis large enough to "whole body" count a PMT in this fashion. This facility will also be used to count a reference PMT, which will then be crushed and counted again for better accuracy. In this way a conversion factor from crushed to whole body counts can be obtained and used to ensure radiopurity quality during the manufacturing process. Capacitors and other components of the PMT base will be radioassayed as well. This radioassay work will be performed by U.C. Davis and by Sandia using LBNL facilities.

5.3 Check with a Detailed MC

GEANT3 and GEANT4 based simulations have been built for estimating the expected singles rate spectrum for the activities shown in Table 15. In addition, an event generator has been written that includes all the known gamma lines from ^{40}K, ^{208}Tl, and ^{214}Bi decay. These are the major radioactive species that could produce events above our threshold of about 0.7 MeV. Table 17 shows the singles rates expected from various detector components. The "high" and "low" designations refer to the highest and lowest radiopurities found in the literature, which gives an idea of the spread of possible values.

Thus we expect the background rate in Double Chooz at 1 MeV to be a factor of roughly twenty less than Chooz at 1.3 MeV. Assuming a neutron-like event rate of 90 per hour (based on the Chooz experience), an average value for the internal activity, and a 100 μs coincidence window, this translates into a random coincidence rate of about one per day in the Double Chooz far detector.

5.4 Radiopurity Monitoring

To ensure that the sensitivity goal of the Double Chooz experiment is attained, great care must be taken to keep the background trigger rate at or below the design level of a few Hz. This in turn requires that great care be taken in material selection, so that the intrinsic radioactivity of detector components does not produce too high a background rate. We will undertake a comprehensive radioactivity survey of the materials that will be used in Double Chooz to ensure that all components will meet or exceed the required level of radiopurity. This survey will also prove useful to other types of highly sensitive experiments, including those searching for neutrinoless double beta decay and dark matter.

Activity measurements requiring very high sensitivity will be made at the Oroville Low Background Counting Facility. This facility, operated by the Lawrence Berkeley National Laboratory, is located in the powerhouse of the Oroville Dam in Northern California, under 180 m of rock cover (600 m.w.e.). It has three Ge spectrometers: a 115% n-type, an 80% p-type, and a 30% p-type. Sensitivities of 50 parts per trillion (PPT) for U and daughters, 200 PPT for Th and daughters, and 100 PPB for K are realized. This is sufficient for checking the activity of the acrylic used in vessel construction.

Activity measurements requiring less precision (such as PMT glass and steel) can also be made in a new facility to be built at U.C. Davis with university funds. This facility will also be able to count large components (such as entire PMTs) to the required level of activity.

Sandia National Laboratories will manage this survey, collecting samples from the various groups building detector components, coordinating counting with U.C. Davis and LBNL, and analyzing and summarizing the results. All materials to be used in Double Chooz will have to be validated in this way. We estimate the need to count roughly sixty samples before or during construction. Table 18 shows the current sampling list. Large items and those that are close to or in contact with the target or gamma catcher scintillator require high sensitivity counting. As one moves further from the active volumes, the radiopurity requirements become less stringent.

System	Component	Sensitivity required	Est. number
Target	Acrylic tank	high	2
	z-axis cable	low	2
	Calibration source soak liquids	low	10
	Acrylic glue	medium	2
	Laser fiber	high	2
	Scintillator	high	2
Gamma Catcher	Acrylic tank	high	2
	Source guide tube	medium	2
	Acrylic glue	medium	2
Buffer	Buffer tank steel	medium	2
	Welding rods	medium	2
	PMTs	medium	10
	PMT mount steel	medium	2
	PMT mu-metal	medium	2
	PMT mounting hardware	medium	2
	Inner PMT cables	medium	2
	PMT Base circuitry and potting	medium	2
Inner Veto	Mounting hardware	low	2
	PMT mounts	low	2
	PMT cables	low	2
	Tank steel	low	2
	Welding rods	low	2
Other	Shield steel	low	2
	Rock	low	2
Total			64

Table 18: Sample list for verification of detector materials. High sensitivity materials will be counted at the LBNL Oroville facility. Medium and Low sensitivity may be counted at either the LBNL or U.C. Davis sites.

References

[1] F. Ardellier et al., "Double Chooz: A Search for the Neutrino Mixing Angle θ_{13};" hep-ex/0606025. This is referred to as the Full Collaboration Double Chooz Proposal in this document.

[2] F. Ardellier et al., "Letter of Intent for Double-CHOOZ: a Search for the Mixing Angle θ_{13};" hep-ex/0405032.

[3] S. Berridge et al., "Proposal for U.S. participation in Double-CHOOZ: A New θ_{13} Experiment at the Chooz Reactor"; hep-ex/0410081.

[4] K. B. M. Mahn and M. H. Shaevitz, "Comparisons and Combinations of Reactor and Long-Baseline Neutrino Oscillation Measurements," hep-ex/0409028.

[5] P. Huber, M. Lindner, T. Schwetz, and W. Winter, "Reactor neutrino experiments compared to superbeams," Nucl. Phys. B**665**, 487 (2003).

[6] H. Minakata, H. Sugiyama, O. Yasuda, K. Inoue, and F. Suekane, "Reactor measurement of θ_{13} and its complementarity to long-baseline experiments," Phys. Rev D**68**, 033017 (2003).

[7] Talk by John Cooper at the FNAL PAC meeting, June 18–19, 2005; http://www-nova.fnal.gov/

[8] The White Paper, "A New Nuclear Reactor Neutrino Experiment to Measure θ_{13}" is available at http://www.hep.anl.gov/minos/reactor13/white.html; also hep-ex/0402041.

[9] J. C. Anjos et al., "Angra Neutrino Project;" hep-ex/0511059.

[10] Y. Wang, Int. J. Mod. Phys. A **20** (2005) 5244.

[11] M. Kuze et al., "The KASKA project – a Japanese medium-baseline reactor-neutrino oscillation experiment to measure the mixing angle θ_{13};" hep-ex/0502002.

[12] For a discussion of RENO, see the next reference.

[13] M. Goodman, "Low Energy Neutrinos," presented to the ICFA workshop in Daegu, South Korea, 28 Sep 2005; http://www.hep.anl.gov/mcg/goodmankorea.ppt.

[14] P. Huber and T. Schwetz, Phys. Rev. D **70** 053011 (2004).

[15] M. Apollonio et al., Eur. Phys. J. C **27** 331, (2003).

[16] P. Antonioli et al., Astropart. Phys. **7**, 357 (1997).

[17] A. Baldini et al., *Geology at the CHOOZ site*, 1995 (unpublished).

[18] A. Tang, talk given at the MAND-sim Workshop in Kansas State University, Manhattan, KS (June 2005). See `http://neutrino.phys.ksu.edu/MAND-sim/MAND-sim%20talks` for a file labelled `DayaBay_ksutalk.pdf`.
A.Tang et al., *Muon simulations for Super-Kamiokande, KamLAND and Chooz*, Phys. Rev. D74 053007 (2006).

[19] PDG Reviews of Particle Properties, Phys. Lett. B 592 (2004).

[20] J. W. F. Valle, hep-ph/0509262.

[21] We are grateful to Hamamatsu Corporation for providing results of their measurements of the R5912 phototube.

[22] http://www.ngdc/noaa.gov/seg/geomag/jsp/struts/calcPointIGRF.

[23] T. Lagomarsino and G. Testera, Nucl. Instrum. Meth. A **430** 435 (1999).

[24] V. A. Kudryavtsev et al., Energy calibration of large underwater detectors using stopping muons, Phys. Lett. B 494 175 (2000).

[25] `http://www.maxim-ic.com/1-Wire.cfm`.

[26] `http://www.ibutton.com/weather/`.

[27] `http://www.sunnuclear.com/products/radon/radon.asp`.

[28] Honeywell HMC2003 datasheet, `http://www.ssec.honeywell.com/magnetic/datasheets/h`

[29] "Future Neutrino Detectors and their Impact on Particle- and Astrophysics," Christian Grieb, Dissertation, Technische Universitaet Muenchen (2004).